Cryptic patterns of speciation in cryptic primates: microendemic mouse lemurs and the multispecies coalescent

Running title: Cryptic speciation in mouse lemurs

Dominik Schüßler[1#], Jordi Salmona[2#], Marina B. Blanco[3,4#], Jelmer Poelstra[4#], George P. Tiley[4#], Jean B. Andriambeloson[5], Olivier Bouchez[6], C. Ryan Campbell[4†], Paul D. Etter[7], Amaia Iribar[2], Paul A. Hohenlohe[8], Kelsie E. Hunnicutt[4@], Eric A. Johnson[7], Peter A. Larsen[4&], Jasmin Mantilla-Contreras[1], Sophie Manzi[2], Alexandra Miller[9], Blanchard Randrianambinina[10,11], David W. Rasolofoson[10], Amanda R. Stahlke[8], David Weisrock[12], Rachel C. Williams[3,4], Lounès Chikhi[2,9], Edward E Louis Jr.[13], Anne D. Yoder[4]*, Ute Radespiel[14]*

[1]: Research Group Ecology and Environmental Education, Institute of Biology and Chemistry, University of Hildesheim, Universitaetsplatz 1, 31141 Hildesheim, Germany

[2]: CNRS, Université Paul Sabatier, IRD; UMR5174 EDB (Laboratoire Évolution & Diversité 11 Biologique), 118 route de Narbonne, 31062 Toulouse, France

[3]: Duke Lemur Center, Duke University, Durham, NC 27705, USA

[4]: Department of Biology, Duke University, Durham, NC 27708, USA

[5]: Zoology and Animal Biodiversity, University of Antananarivo, Antananarivo 101, Madagascar

[6]: INRA, US 1426, GeT-PlaGe, Genotoul, Castanet-Tolosan, France

[7]: Institute of Molecular Biology, University of Oregon, Eugene, OR, USA

[8]: Institute for Bioinformatics and Evolutionary Studies, Department of Biological Sciences, University of Idaho, Moscow, ID 83844, USA

[9]: Instituto Gulbenkian de Ciência, Rua da Quinta Grande, 6, 2780-156 Oeiras, Portugal

[10]: Groupe d'Etude et de Recherche sur les Primates de Madagascar (GERP); BP 779, Antananarivo 101, Madagascar

[11]: Faculté des Sciences, University of Mahajanga, Mahajanga, Madagascar

[12]: Department of Biology, University of Kentucky, Lexington, KY, 40506, USA

[13]: Grewcock Center for Conservation and Research, Omaha's Henry Doorly Zoo and Aquarium, Omaha, NE

[14]: Institute of Zoology, University of Veterinary Medicine Hannover, Buenteweg 17, 30559 Hannover, Germany

#: joint first authors

*: joint senior authors (corresponding authors)

@: current address: Department of Biological Sciences, University of Denver, Denver, CO 80208

&: current address: Department of Veterinary and Biomedical Sciences, University of Minnesota, Saint Paul, MN 55108

†: current address: Department of Evolutionary Anthropology, Duke University, Durham, NC 27708, USA

Corresponding authors:

Ute Radespiel, Institute of Zoology, University of Veterinary Medicine Hannover, Germany, email: ute.radespiel@tiho-hannover.de

Anne D. Yoder, Department of Biology, Duke University, Durham, NC, USA, email: anne.yoder@duke.edu

Author contributions:

- *Conception and design of study:*

DS, JS, LC, JP, GPT, JMC, ADY, UR

- *Data collection:*

DS, MBB, JBA, AM, EELJ, DWR, BR collected samples in the field.

- *Data analysis and interpretation:*

DS, JS, LC, OB, PE, CRC, PAL, ARS, DW, AIP, PH, KEH, EJ, SM, RCW, EELJ, UR generated sequencing data.

DS, JS, MBB, JP, GPT, ADY, UR conducted and interpreted morphometric, population genetic and phylogenetic analyses.

- *Drafting and revising manuscript:*

DS, JS, JP, GPT, ADY, UR drafted the manuscript.

All co-authors revised and agreed on the last version of the manuscript.

Abstract

Species delimitation is ever more critical for assessing biodiversity in threatened regions of the world, with cryptic species and rapid radiations offering two of the greatest challenges, especially when they occur in conjunction. Mouse lemurs (*Microcebus*) are an example of a rapid, cryptic radiation and here we study five phylogenetic lineages that are found within a restricted geographic area in northeastern Madagascar. To delimit and characterize species diversity we utilize a conceptual framework based on the multispecies coalescent (MSC). Morphometric analyses reveal only minute phenotypic differences among lineages, thus confirming the cryptic nature of taxa. By analyzing genome-wide SNP data, we assess effective population sizes (N_e), divergence times, and patterns of gene flow to inform hypotheses of species delimitation in the context of geographic distribution, ecology and morphological distinction. Differences in N_e have a significant impact on MSC-based species delimitation, particularly with regard to the recently introduced genealogical divergence index (*gdi*). Lineages with low N_e pass the heuristic *gdi* test while high N_e lineages fail to delimit a previously recognized species pair. Further, we find that incorporating gene flow into the MSC can greatly affect divergence time estimates. Even so, we are confident that speciation occurred recently and rapidly in this cryptic radiation with reproductive isolation apparent from two areas where divergent lineages occur sympatrically. Finally, we conclude that a previously identified mitochondrial lineage warrants full species status, and provide a species description for this lineage, naming it *M. jonahi*. Alarmingly, analyses of both whole-genome and RADseq data show a precipitous decline in N_e in this newly described microendemic, thus indicating a high risk of extinction even in the moment of its recognition as a new species.

Keywords: effective population size, *Microcebus jonahi*, cryptic species, multispecies coalescent, species delimitation, speciation, microendemism

Introduction

The accurate delimitation of species is essential to the investigation of evolutionary mechanisms as well as for estimating the extent of global biodiversity. It is increasingly acknowledged that cryptic species are "the elephant in the room" for correctly assessing these parameters (Adams et al. 2014). There have been recent calls for a conceptual framework for identifying cryptic species (Struck et al. 2018) and for properly integrating them into biodiversity science, including formal species description with appropriate taxonomy (Fiser et al. 2017). Here, we follow these guidelines for assessing species diversity in mouse lemurs (genus *Microcebus*) from a restricted geographic region in Madagascar of intense conservation concern.

Given that cryptic species are by definition difficult to identify based on phenotypic variation (Struck et al. 2018), rapidly developing methods for genomic species delimitation have profoundly advanced our ability to recognize and quantify species diversity. In the past decade, both theory and methods for species delimitation have seen substantial progress and stimulating debate, especially those which leverage the multispecies coalescent (MSC) model (Pamilo and Nei 1988; Rannala and Yang 2003). Relying on molecular data and MSC-based species delimitation methods (e.g. Yang and Rannala 2010; Carstens and Dewey 2010; Grummer et al. 2013) has been deemed controversial (Edwards and Knowles 2014; Barley et al. 2017; Sukumaran and Knowles 2017), largely because the alternative hypothesis of strong population structure when assigning species boundaries is not considered (Jackson et al. 2017; Sukumaran and Knowles 2017; Luo et al. 2018; Chambers and Hillis 2019; Leaché et al. 2019). To overcome this potential weakness, Jackson et al. (2017) proposed a heuristic criterion, the genealogical divergence index (*gdi*), with Leaché et al. (2019) further suggesting that *gdi* helps to differentiate

115 between population structure and species-level divergence. In parallel, sophisticated statistical
116 approaches that can detect the presence and magnitude of gene flow before or after speciation
117 events have been developed (Gronau et al. 2011; Payseur and Rieseberg 2016; Dalquen et al.
118 2017; Wen et al. 2018). Taken together, these analytical developments are crucial to our ability to
119 recognize the patterns that characterize the speciation process, despite the challenge of
120 identifying species without universally agreed upon criteria (de Queiroz 2007).
121
122 Mouse lemurs (*Microcebus* spp.) are small and nocturnal primates inhabiting remote and
123 highly threatened areas of Madagascar, one of the world's most biodiverse environments (Myers
124 et al. 2000; Goodman and Benstead 2005; Waeber et al. 2016; Estrada et al. 2017). These
125 primates have been shown to represent a notoriously problematic group for robust species
126 delimitation (Hotaling et al. 2016) given that they exhibit patterns of rapid diversification, cryptic
127 morphology, and overlapping geographic distributions (e.g., Zimmermann et al. 1998;
128 Rasoloarison et al. 2000; Radespiel et al. 2008). Furthermore, the existing lack of phylogenetic
129 consensus among previous studies (Weisrock et al. 2010; Hotaling et al. 2016; dos Reis 2018)
130 may be due to rapid and recent lineage diversification, thus placing them in the "anomaly zone"
131 wherein species trees feature short branch lengths between speciation events, and accordingly,
132 high discordance among gene trees as a function of incomplete lineage sorting (Degnan and
133 Rosenberg 2006). Mouse lemur diversity was long overlooked (Zimmermann and Radespiel
134 2014) until the introduction of genetic analyses made it feasible to identify diverging lineages
135 despite similar phenotypes and roughly similar ecological niches. This genetic perspective has led
136 to the description of many new species, most of them from the western part of the island
137 (Zimmermann et al. 1998; Rasoloarison et al. 2000; Yoder et al. 2000; Louis et al. 2008; Olivieri
138 et al. 2007) with eastern regions only recently receiving increased levels of attention to the

possibility of novel species (Kappeler et al. 2005; Louis et al. 2006; Radespiel et al. 2008, 2012; Rasoloarison et al. 2013; Hotaling et al. 2016).

In particular, Radespiel et al. (2008) surveyed the forests of the Makira region (Fig. 1) and found evidence for three diverged lineages occurring in sympatry, a phenomenon previously undocumented for mouse lemurs. One of these was identified as *M. mittermeieri*, while the second was newly described as *M. macarthurii*. A third lineage (*M.* sp. #3) was hypothesized to be a new species based on mitochondrial DNA (mtDNA) sequence data but could not be formally described given that only a single individual was sampled. Our study takes advantage of increased geographic and population-level sampling to fully explore this hypothesis.

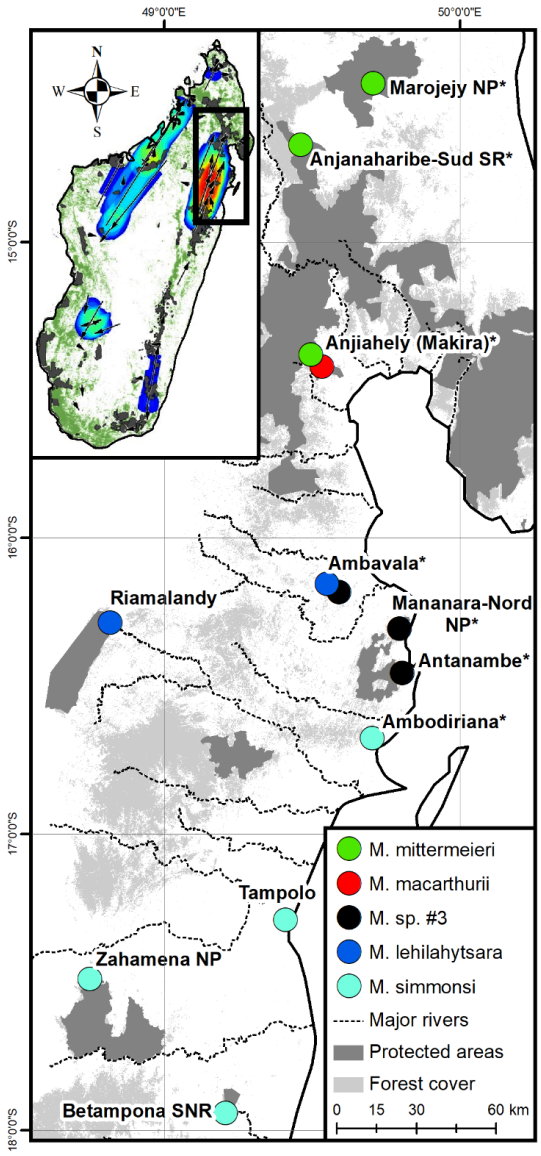

Figure 1: Sampling sites in northeastern Madagascar. New sampling locations are marked with *. The region coincides with a conservation hotspot for lemurs (see heat map in the inlay with warm colors representing conservation concern based on predicted range shifts in a large number of lemur species reproduced from Brown and Yoder 2015). Forest cover in 2018 derived from Schüßler et al. (in revision).

Many previous taxonomic descriptions have relied strongly, if not entirely, on mitochondrial sequence divergence to delimit the presently 24 recognized mouse lemur species (Hotaling et al. 2016), prompting criticism in terms of “taxonomic inflation” and "oversplitting" of linages (Tattersall 2007; Markolf et al. 2011). Indeed, the mtDNA approach to species

160 recognition is widely regarded as problematic, given that the mitogenome represents only a
161 single, non-neutral, non-recombining locus whose gene tree may not represent the underlying
162 species tree (e.g., Pamilo and Nei 1988; Maddison 1997). Mitochondria are also maternally
163 inherited and therefore susceptible to effects of sex-biased dispersal (e.g., Dávalos and Russell
164 2014), which is prevalent in mouse lemurs (Radespiel et al. 2001). To further complicate matters,
165 previous attempts to resolve relationships using sequences from nuclear markers were
166 complicated by high gene tree discordance consistent with strong incomplete lineage sorting
167 (e.g., Heckman et al. 2007; Weisrock et al. 2010). But now, with genomic approaches,
168 investigators can sample thousands of loci across multiple individuals, which provides power for
169 simultaneously resolving phylogenetic relationships and for estimating demographic parameters
170 such as divergence times, effective population sizes, and rates of gene flow — even among
171 closely related species (e.g., Palkopoulou et al. 2018; Pedersen et al. 2018).
172
173 In this study, we utilize a conceptual framework to comprehensively delimit species under
174 complex patterns of speciation, including rapid diversification, cryptic species richness, and
175 incomplete linage sorting. To exemplify our approach, we revisit the Radespiel et al. (2008)
176 findings by expanding the geographic and species-level sampling to reconstruct the evolutionary
177 history of the mouse lemur lineages inhabiting this region and to test the hypothesis that *M.* sp.
178 #3 actually represents a new species. We also provide a novel whole genome for this
179 hypothesized new species thus allowing for a detailed conservation genomic analysis. Our study
180 therefore represents the most intensive examination to date of speciation dynamics within this
181 cryptic species radiation.
182
183 **Analytical framework**

We utilize a conceptual framework that can be applied to any biological system that requires evaluation of its species diversity under threat from habitat loss and fragmentation – even under complicated conditions of rapid speciation and ambiguous morphological differentiation. Our general approach is summarized in Figure 2 with a workflow that is composed of four successive steps: (A) thorough geographic sampling and analyses of phenotypic divergence, (B) mtDNA barcoding, (C) phylogenetic placement of focal lineages, and (D) use of genomic data for MSC analyses.

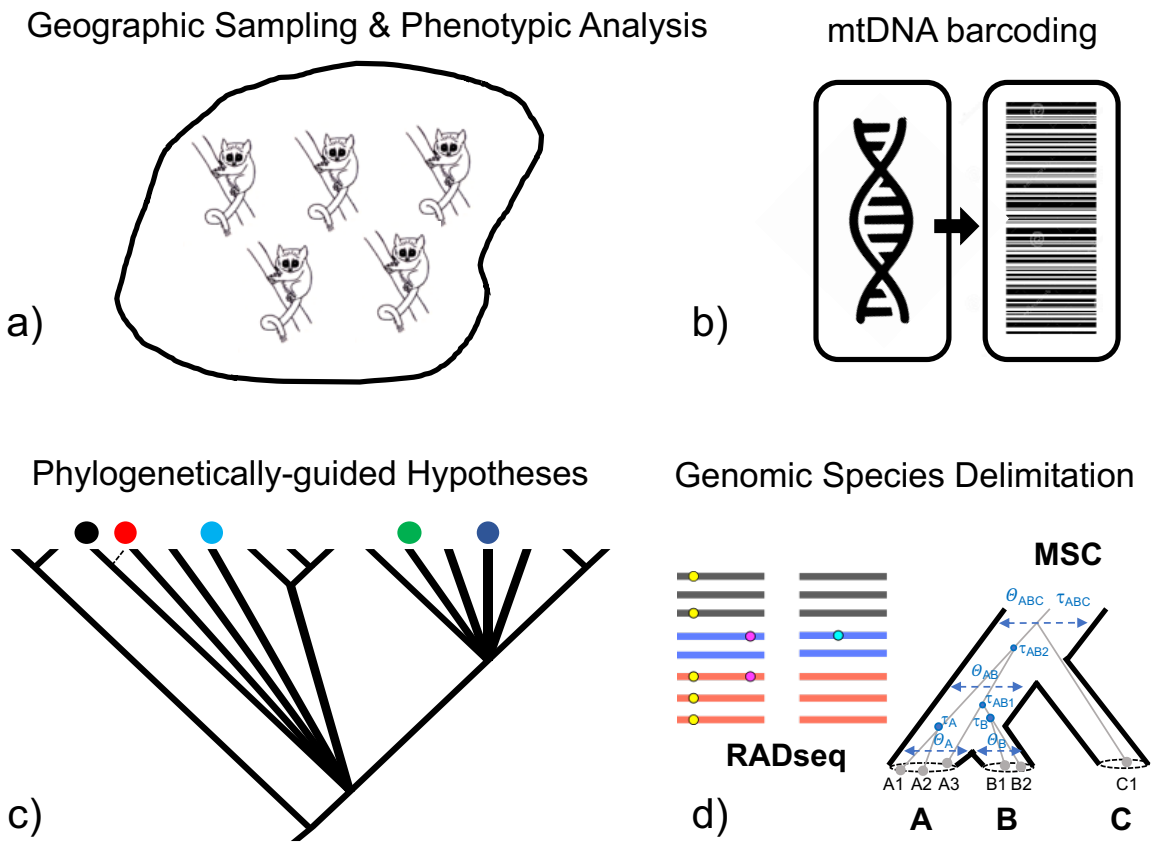

Figure 2: A structured approach for assessing mouse lemur species diversity in a restricted geographic area. (A) Thorough sampling of relevant populations accompanied by phenotypic analysis to assure adequate geographic coverage and estimation of cryptic diversity. **(B)** DNA barcoding to assign

individuals to previously hypothesized species lineages based on published data, allowing for subsequent detection of co-occurrence in sympatry. **(C)** Prior knowledge of phylogenetic proximity is used to guide multispecies coalescent study design (colored circles correspond to those in Figure 1). **(D)** Development of further genomic resources (in our case, genome-wide SNP data generated via RADseq) to enhance the power of species delimitation methods using the multispecies coalescent (redrawn from Figure 1 in Fujita et al. (2012)).

Materials and methods

Study sites and sampling

Microcebus individuals were sampled between 2008 and 2017 at seven rain forest sites (50-979 m a.s.l.; Kottek et al. 2006) in the Analanjirofo and Sava regions of northeastern Madagascar (Fig. 1; Tab. S1). All study sites harbor a variety of habitats ranging from undisturbed near-primary rain forest to heavily degraded secondary shrub-, grass- and fern-lands (Radespiel et al. 2008; Miller et al. 2018; Schüßler et al. 2018). Additional samples were used from Riamalandy, Zahamena National Park (NP), Betampona Strict Nature Reserve (SNR) and Tampolo (Louis et al. 2006; Weisrock et al. 2010; Louis and Lei 2016; Fig. 1). With this sampling strategy, we expect to detect all mouse lemur species that occur in the region. These are (from north to south) *M. mittermeieri*, *M. macarthurii*, *M*. sp. #3, *M. lehilahytsara* and *M. simmonsi* (Fig. 1). *Microcebus murinus,* which occurs throughout western and southern Madagascar, was used as an outgroup for the analyses.

Morphometric analyses

We measured 13 different morphometric parameters (ear length, ear width, head length, head width, snout length, inter- and intra-orbital distance, lower leg length, hind foot length, third toe length, tail length, body length and body mass) according to Hafen et al. (1998) and Zimmermann et al. (1998). Individuals were assigned to their respective taxon based on phylogenetic and clustering analyses. The morphological data of all captured and released adult mouse lemurs were compared among species and with data sets available from geographically neighboring species (Fig. 1). A linear discriminant analysis (LDA) was conducted to test for species differentiation based on morphometrics using the “MASS” package (v7.3-51.3; Venables and Ripley 2002) in R (R Core Development Team 2013). Model fit was evaluated by a jackknife

227 cross-validation and Wilks' Lambda was computed to evaluate the LDA model. R^2 values were
228 calculated using the "flipMultivariates" package (Displayr 2018) to document the proportion of
229 variance per parameter that is explained by the species. Quantitative morphometric comparisons
230 between taxa were performed for all measurements with a one-way ANOVA and a post hoc
231 Tukey test. Assumptions of the respective tests were examined using Shapiro-Wilk and Levene's
232 tests in the R package car v3.0-2 (Fox and Weisberg 2011) beforehand.
233
234 One limitation to the morphometric analyses is that body measurements of the different taxa
235 were obtained by at least four researchers across the five different lineages, and it cannot be ruled
236 out that researchers may have differed slightly in how they applied the calipers. However, the
237 same researcher contributed data points to more than one species in at least two cases (DS,
238 DWR).
239
240 **RADseq laboratory procedures and data processing**
241 We generated Restriction site Associated DNA sequencing (RADseq) libraries using the
242 *Sbf*I restriction enzyme, following three protocols (Supplementary Methods, `Tab. S1`). Cleaned
243 sequences were aligned to *M.* sp. #3 genome and to the *M. murinus* mitogenome (Lecompte et al.
244 2015; see Supplementary Methods for further details).
245
246 We used two fundamentally distinct approaches for genotyping to ensure robustness of our
247 results to variant calling errors. First, we estimated genotype likelihoods (GL) with ANGSD
248 v0.92 (Nielsen et al. 2012; Korneliussen et al. 2014). ANGSD retains information about
249 uncertainty in base calls, which alleviates some issues commonly associated with RADseq data
250 such as unevenness in sequencing depth and allele dropout (Lozier 2014; Pedersen et al. 2018;

251 Warmuth and Ellegren 2019). Second, we called genotypes with GATK v4.0.7.0 (dePristo et al.
252 2011), and filtered GATK genotypes following the "FS6" filter of O'Leary et al. (2018; see
253 Supplementary Methods for further details).
254
255 Three mtDNA fragments [Cytochrome Oxidase II (COII), Cytochrome B (cytB), d-loop]
256 were amplified and Sanger sequenced for additional phylogenetic analyses. For further details on
257 sequencing and genotyping procedures, see the Supplementary Material.
258
259
260 **Phylogenetic analyses**
261 We used three phylogenetic approaches to infer relationships among lineages and to provide
262 a framework for subsequent species delimitation analyses. Phylogenetic analyses were conducted
263 via (1) maximum likelihood (RaxML v8.2.11; Stamatakis 2014), (2) a MSC method that is
264 statistically consistent and uses phylogenetic invariants (SVDquartets in PAUP v4a163; Chifman
265 and Kubatko 2014), and (3) a full-likelihood MSC method for biallelic data that does not require
266 joint gene tree estimation (SNAPP v1.3.0; Bryant et al. 2012). Analyses with RAxML and
267 SVDquartets used all available individuals, whereas SNAPP analyses were only performed with
268 subsets of individuals for computational feasibility. Specifically, a 12-individual dataset that used
269 two samples per species, and a 22-individual dataset with four samples per species were analyzed
270 with SNAPP (Tab. S1). All analyses used *M. murinus* samples as outgroup. Phylogenetic
271 software details are given in the Supplementary Material.
272
273 **Sequencing, assembly, and annotation of a *M.* sp. #3 draft genome**

274 The genome of one individual of *M*. sp. #3 sampled from Mananara-Nord NP (Tab. S2)
275 was sequenced with a single 500bp insert library on a single lane of an Illumina HiSeq 3000 with
276 paired-end 150bp reads. Similarly, the genome of *M*. *mittermeieri* was sequenced as
277 approximately 400bp insert libraries on a single lane of an Illumina HiSeq 3000 with paired-end
278 150bp reads (Hunnicutt et al., 2019). We used MaSuRCA v3.2.2 (Zimin et al. 2013) for contig
279 assembly and SSPACE (Boetzer et al. 2011) for scaffolding, which uses BOWTIE (Langmead et
280 al. 2009) to realign short reads to the *de novo* assembly in order to potentially correct erroneously
281 joined contigs. Quality control and annotation of the draft genome is described in the
282 Supplementary Material. Scaffolds potentially containing mitochondrial or X-chromosome
283 sequence data were removed for downstream analyses (see Supplementary Methods).
284
285 **RADseq laboratory procedures and data processing**
286 We generated Restriction site Associated DNA sequencing (RADseq) libraries using the *Sbf*I
287 restriction enzyme, following three protocols (Supplementary Methods, Tab. S1). Cleaned
288 sequences were aligned to *M.* sp. #3 genome and to the *M. murinus* mitogenome (Lecompte et al.
289 2015; see Supplementary Methods for further details).
290
291 We used two fundamentally distinct approaches for genotyping to ensure robustness of our results
292 to variant calling errors. First, we estimated genotype likelihoods (GL) with ANGSD v0.92
293 (Nielsen et al. 2012; Korneliussen et al. 2014). ANGSD retains information about uncertainty in
294 base calls, which alleviates some issues commonly associated with RADseq data such as
295 unevenness in sequencing depth and allele dropout (Lozier 2014; Pedersen et al. 2018; Warmuth
296 and Ellegren 2019). Second, we called genotypes with GATK v4.0.7.0 (dePristo et al. 2011), and

filtered GATK genotypes following the "FS6" filter of O'Leary et al. (2018; see Supplementary Methods for further details).

Three mtDNA fragments [Cytochrome Oxidase II (COII), Cytochrome B (cytB), d-loop] were amplified and Sanger sequenced for additional phylogenetic analyses. For further details on sequencing and genotyping procedures, see the Supplementary Material.

Mutation rate and generation time

To convert coalescent units from BPP and G-PhoCS analyses into absolute times and population sizes, we used empirical estimates of mutation rate and generation time but used uncertainty in estimates to construct distributions rather than using a single point estimate for BPP and G-PhoCS results. For each sampled generation of the MCMC chain, we drew a random number from the mutation rate and generation time distributions to better reflect our uncertainty in absolute estimates. A recent pedigree-based estimate of mutation rate in *M. murinus* (Campbell et al. 2019) found a mean of 1.64×10^{-8} with a 95% CI of 1.41×10^{-8} to 1.98×10^{-8}. We roughly capture this mutation rate variation with a normal distribution that has a mean of 1.64 and a standard deviation of 0.08. For generation time, two estimates were available for *Microcebus*. *M. rufus* was estimated to have an average generation time of 4.5 years calculated from survival data (Zohdy et al. 2014; Yoder et al. 2016), and 2.5 years was estimated for *M. murinus* using average parent age based on capture-mark-recapture and parentage data in the wild (Radespiel et al. 2019). We used a lognormal distribution with a mean of ln (3.5) and standard deviation of ln (1.16). MSMC parameter estimates were converted using the point estimates.

Species delimitation

Model-based inference with the MSC

We used SNAPP to test if the two pairs of sister taxa, *M.* sp. #3 – *M. macarthurii* and *M. mittermeieri* – *M. lehilahytsara*, could be delimited at the molecular level using Bayes factors (Leaché et al. 2014). Marginal likelihood estimation used stepping-stone sampling (Xie et al. 2011) with 20 steps for both the 12- and 22- individual datasets, and we interpreted 2ln Bayes factors greater than six as strong evidence for a given model (Kass and Raftery 1995). We tested two hypotheses: the first considered the two taxa in each species pair as separate species, and the second considered them as belonging to the same species.

We also applied guided species delimitation analyses with BPP (Yang and Rannala 2010; Rannala and Yang 2013) based on the species tree estimated by SVDquartets and SNAPP but using analytical integration of population sizes (Hey and Nielsen 2007). MCMC options and prior choices for analyses are detailed in the Supplementary Material. Because BPP uses substitution models not suitable for SNP data, we created full sequence fasta files based on the GATK genotypes using a series of in-house scripts (https://github.com/jelmerp/msp3/tree/master/vcf2fullfasta; Supplementary Material).

BPP parameter estimates from the 12-individual dataset with the MSC were used to compute the genealogical divergence index (*gdi*, Jackson et al. 2017; Leaché et al. 2019) for *M.* sp. #3 – *M. macarthurii* and *M. lehilahytsara* – *M. mittermeieri*. We calculated *gdi* as in Leaché et al. (2019), using their equation 7 ($gdi = 1-e^{-2\tau/\theta}$), where $2\tau/\theta$ represents the population divergence time between taxa A and B in coalescent units, and θ is taken for a focal taxon (A or B). Again, as in Leaché et al. (2019), *gdi* was calculated twice for each species pair, using each species as the focal taxon once. We computed *gdi* using τ and θ parameter estimates for each posterior sample

345 from independent BPP chains, to directly incorporate uncertainty in the τ and θ estimates.
346 Jackson et al. (2017) suggested the following guidelines for the interpretation of *gdi* values: the
347 focal taxon pair is unambiguously a single species for *gdi* < 0.2, is unambiguously two separate
348 species for *gdi* > 0.7, and falls in an ambiguous zone for 0.7 > *gdi* < 0.2.
349
350 *Clustering approaches and summary statistics*
351 We performed model-based as well as naive clustering analyses in order to check for
352 congruence with phylogenetic analyses, to identify intraspecific genetic structure, and to perform
353 an initial exploration of gene flow or admixture between species. Clustering analyses were
354 performed using corresponding methods based on ANGSD genotype likelihoods [clustering in
355 NgsAdmix v32 (Skotte et al. 2013) and PCA in ngsTools va4d338d (Fumagali et al. 2013, 2014)],
356 on GATK-called genotypes (ADMIXTURE v1.3.0; Alexander et al. 2009) and glPca (adegenet
357 v2.1.1; Jombart 2008; Jombart and Ahmed 2011). These analyses were run separately for all
358 successfully sequenced samples for the five focal taxa (`Tab. S1`) and for a subset comprising
359 only individuals from *M. macarthurii* and *M.* sp. #3. Heterozygosity and F_{ST} were estimated with
360 the R packages adegenet v2.1.1 (Jombart 2008) and hierfstat (Goudet 2005) on variable sites
361 inferred from ANGSD for comparison with clustering results.
362
363 **Inference of interspecific gene flow**
364 The D-statistic and related formal statistics for admixture make use of phylogenetic
365 invariants to infer post-divergence gene flow between non-sister populations or taxa. However, it
366 is important to note that the D-statistic may also be influenced by ancient population structure
367 and should thus be interpreted with care (Eriksson and Manica 2012; Chikhi et al. 2018). We
368 used admixtools v4.1 (Patterson et al. 2012) to compute four-taxon D-statistics (qpDstat

369 program), which tests for gene flow between P3 and either P1 or P2 given the topology (((P1,
370 P2), P3), P4). In order to test for gene flow between *M. macarthurii* and *M.* sp. #3, we separately
371 treated (1) the two distinct *M.* sp. #3 population groups detected by clustering approaches, and (2)
372 *M. macarthurii* individuals with and without "*M.* sp. #3-type" mtDNA (see Results). We also
373 used all possible configurations in which gene flow between non-sister species among the five
374 ingroup species could be evaluated. In all tests, *M. murinus* was used as P4 (outgroup).
375 Significance of D-values was determined using the default Z-value reported by qpDstat, which is
376 determined by weighted block jackknifing and is conservative for RADseq data given that
377 linkage disequilibrium (LD) is, on average, expected to be lower across a pair of RADseq SNPs
378 than across a pair of SNPs derived from whole-genome sequencing (Patterson et al. 2012; Kim et
379 al. 2018).
380
381 G-PhoCS v1.3 (Gronau et al. 2011), a Bayesian MSC approach that incorporates
382 introgression, was used to jointly infer divergence times, population sizes, and rates of gene flow
383 between specific lineages. Because running G-PhoCS for all individuals was not computationally
384 feasible, we performed separate runs for two sets of individuals: (1) a 3-species (and 12-
385 individual) data set with six *M.* sp. #3, three *M. macarthurii*, and three *M. lehilahytsara*
386 individuals, wherein *M.* sp. #3 was divided into the two distinct population clusters detected
387 using clustering approaches; and (2) the 5-species (and 12-individual) data set used for SNAPP
388 and BPP. Details of the inference of gene flow are described in the Supplementary Material.
389
390 **Estimation of divergence times**
391 We used two approaches to estimate divergence times under the MSC model: (1) BPP
392 v4.0.4 (Flouri et al. 2018), which assumes no migration after the onset of divergence, and (2) G-

393 PhoCS, which can accommodate migration between specific lineages and co-estimate migration
394 rates and divergence times.
395
396 Both BPP and G-PhoCS analyses used full-length RAD loci from the 12-individual dataset. The
397 species tree recovered from phylogenetic analyses was fixed for parameter sampling. We required
398 at least one individual per species to be present for each locus (on a total of 17,422 RAD loci)
399 and all individuals were treated as unphased diploid sequences. We used diffuse priors, multiple
400 chains, and checked for convergence (Supplementary Material). We also compared posteriors to
401 marginal priors to check that parameter estimates were informed by the RADseq data and not
402 only the priors.
403
404 **Inference of effective population sizes through time**
405 A number of studies have shown that population structure can generate spurious signals of
406 population size change (Beaumont 2004; Chikhi et al. 2010; Heller et al. 2013). For example,
407 sequentially Markovian coalescent approaches such as MSMC actually estimate the inverse
408 instantaneous coalescence rate (IICR), which is only equivalent to an effective size in panmictic
409 models (Mazet et al. 2016; Rodriguez et al. 2018). We therefore inferred and compared
410 population size histories using several methods for the focal species *M.* sp. #3 and for *M.*
411 *mittermeieri*, for which we had whole-genome sequence data in addition to the RADseq data. For
412 all species, we examined changes in N_e over time based on θ estimates from BPP and G-PhoCS
413 for each predefined extant or ancestral population, which also allowed us to evaluate uncertainty
414 in population size estimates due to migration. For *M.* sp. #3 and *M. mittermeieri*, we also
415 estimated N_e over time with the Sequential Markovian Coalescent as implemented in MSMC

(Schiffels and Durbin 2014) using the whole-genome data. A detailed description for these analyses is given in the Supplementary Material.

Results

Morphometric comparisons

Though morphological distinctions are subtle, *Microcebus* sp. #3, *M. macarthurii*, *M. simmonsi* and *M. mittermeieri* can be statistically distinguished based on morphometrics (LDA: Wilks' Lambda = 0.0175, F = 6.7941, P < 0.001; Fig. 3). Apart from ear length, all parameters contributed significantly to species assignments in the LDA model (P < 0.001), with body length and inter-orbital distance having the highest R^2-values (Fig. 3, Tab. S4). Prediction accuracy of the jackknife cross-validated LDA model was 81%. Mis-classifications occurred with *M. simmonsi*, but not between the other three taxa (Tab. S5). All three linear discriminant functions were statistically significant of which the first (LD1) explained 69.3% of interspecific variation and LD2 and LD3 the remaining 23.7% and 7.0%, respectively. *M*. sp. #3 and *M. macarthurii* predominantly differed in five "head-associated" parameters (head width, inter- and intra-orbital distance, snout length, ear width, all larger in *M*. sp. #3) while limb proportions did not show significant differences. We identified three individuals of *M*. *macarthurii* showing mitonuclear discordance (see below) of which two clustered morphometrically with the other *M. macarthurii,* whereas the third was positioned with *M. simmonsi* (Fig. 3).

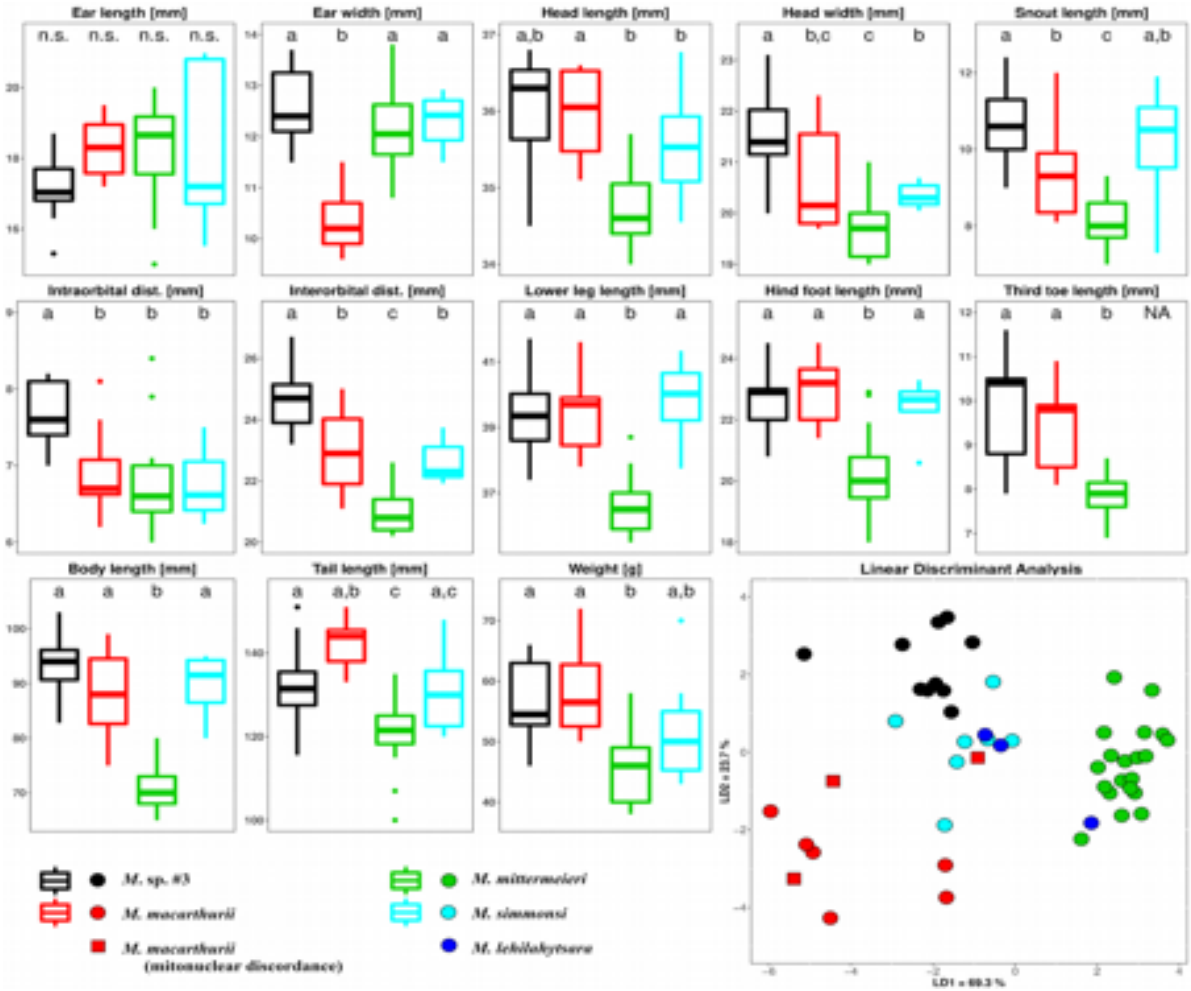

Figure 3: **Interspecific differences in morphometric parameters.**

Small plots: Comparisons based on one-way ANOVA (P < 0.001 for all parameters except ear length) and grouping (letters after values) according to Tukey post-hoc tests. For parameter values, see Table S4. Large plot in bottom right: Linear discriminant analysis (LDA) based on morphometric measurements (M. sp. #3, n = 11; *M. macarthurii*, n = 6; *M. mittermeieri*, n = 22; *M. simmonsi*, n = 7). Individuals of *M. macarthurii* with mitonuclear discordance and of *M. lehilahytsara* were not used to calculate the LDA model due to small sample sizes, their position was predicted using the LDA model (*M. macarthurii*, n = 3; *M. lehilahytsara*, n = 3).

RADseq data and whole genome sequences

This study demonstrates the utility of cross-laboratory RAD sequencing for primates, as previously shown in other taxa (e.g., Gonen et al. 2015). We used three different library

448 generation protocols, two sequencing lengths, and a combination of single and paired-end
449 sequencing, yielding highly compatible data for all 65 individuals included in the study. From
450 more than 447 million raw reads (Tab. S1), over 394 million passed quality filters with
451 approximately 182 million successfully aligned to the *M.* sp. #3 reference genome. There was an
452 average of 120,000 loci per individual with coverage ranging from ~1 to ~22x (Tab. S1).
453
454 We assembled approximately 2.5 Gb of nuclear genome sequence data for *M*. sp. #3 with a
455 contig N50 around 36 Kb (Tab. S2). While the final assembly was fragmented, as expected for
456 a single Illumina library genome, only 6.4% of mammalian BUSCOs were found to be missing.
457 Annotation statistics were largely comparable to BUSCO analysis of the genome assembly. The
458 genome sequence and associated gene annotations can be accessed through NCBI (Bioproject
459 PRJNA512515).
460
461 **Phylogenetic relationships**
462 Five divergent lineages (*M. simmonsi, M. lehilahytsara, M. mittermeieri, M. macarthurii,*
463 *M.* sp. #3) were confirmed to occur in the study region by phylogenetic approaches (Fig. 4).
464 One lineage, *M*. sp. #3, is described here as new to science (see *Species Description*).
465
466 RAxML, SVDquartets, and SNAPP analyses recovered well-supported monophyletic
467 nDNA clades for *M. simmonsi*, *M. macarthurii*, and *M.* sp. #3 (Fig. 4; Fig. S1; Fig. S2),
468 with *M.* sp. #3 as sister to *M. macarthurii* with 100% bootstrap support (RAxML and
469 SVDquartets, Fig. 2; Fig. S2). In contrast, *M. lehilahytsara* and *M. mittermeieri* were not
470 consistently monophyletic in RAxML analyses of nDNA (Fig. 4C) or mtDNA (Fig. 4A),
471 both of which nested *M. mittermeieri* within *M. lehilahytsara*. SVDquartets analysis of nDNA

placed one individual from Ambavala (B12, Fig. 1) as sister to all other *M. lehilahytsara* and *M. mittermeieri* with weak bootstrap support (Fig. S2A). In contrast with the maximum likelihood analysis, species tree analyses with SNAPP (the 22-individual dataset included B12 from Ambavala) recovered *M. lehilahytsara* as sister to *M. mittermeieri* with no topological uncertainty (Fig. S1). We refer to the well-supported *M.* sp. #3 - *M. macarthurii* and *M. mittermeieri* – *M. lehilahytsara* species pairs as Clade I and Clade II respectively.

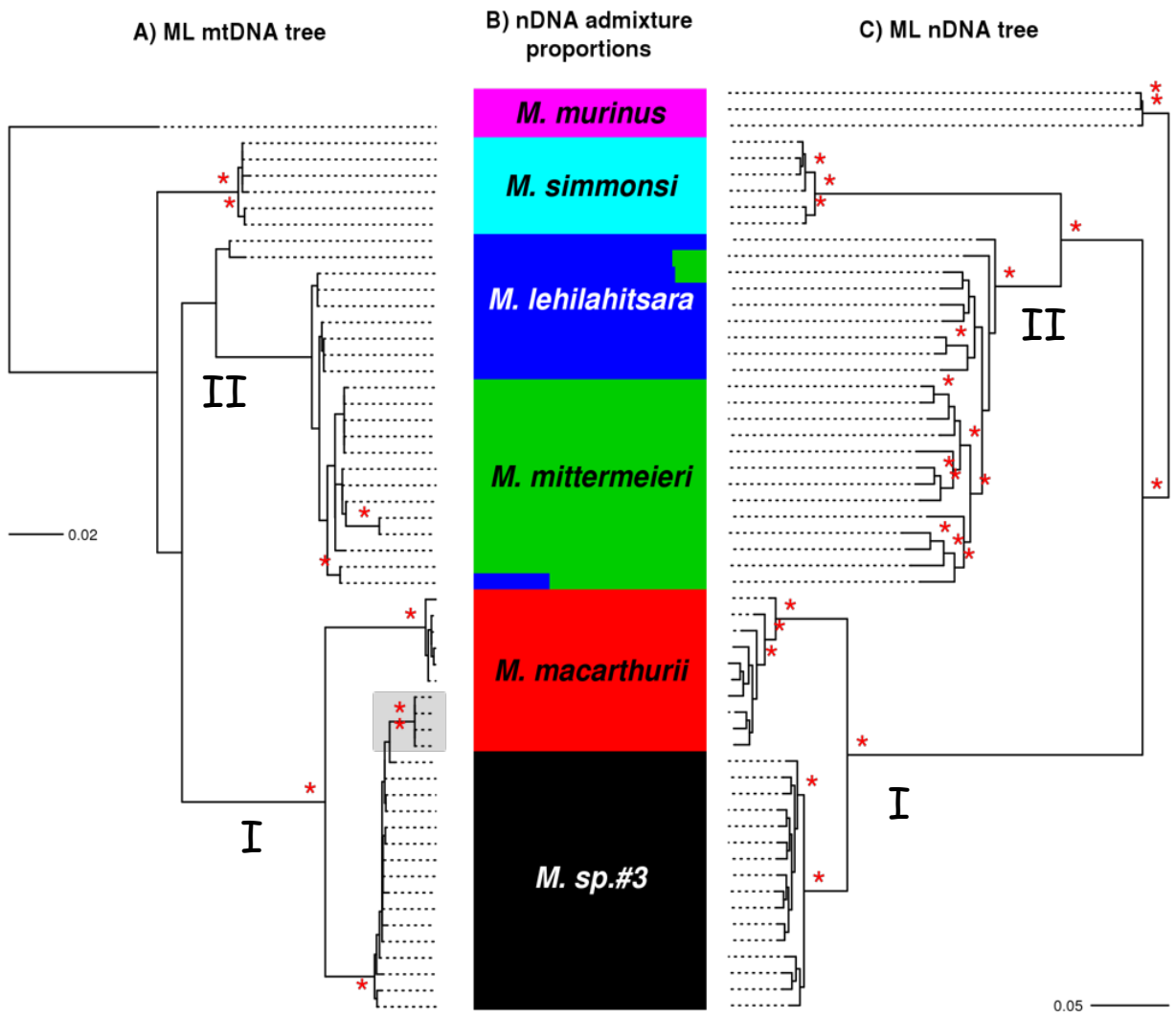

Figure 4: Phylogenetic relationships and ancestry proportions

481 **(A)** Maximum-likelihood RAxML tree of 55 samples represented by 4,060 bp of mtDNA recovered from
482 RADseq and Sanger sequencing (Table S1). The gray shaded box highlights individuals of *M. macarthurii*
483 with *M.* sp. #3 mtDNA haplotypes. **(B)** Clustering results using NgsAdmix at *K* = 6. **(C)** Maximum-likelihood
484 RAXML tree obtained using RADseq nuclear data (nDNA). For all trees, *M. murinus* is used as the
485 outgroup. In **(A)** and **(C)**, bootstrap support values >90% are indicated above each node as a red asterisk.
486 Clade containing species pairs *M. macarthurii* plus *M. sp.*#3 and *M. lehilahytsara* plus *M.* mittermeieri are
487 labeled I and II, respectively, for ease of reference throughout.
488

489 One case of mitonuclear discordance was found. Although mtDNA analyses placed several
490 individuals from Anjiahely (see Fig. 1) in a well-supported clade with *M.* sp. #3 individuals
491 from Ambavala, Mananara-Nord NP and Antanambe (Fig. 4A; see lower red box), analyses of
492 the nuclear RADseq data placed them unambiguously within the *M. macarthurii* clade (Fig.
493 4B,C). This suggests that individuals from Anjiahely belong to *M. macarthurii*, but carry two
494 divergent mtDNA lineages, and that *M.* sp. #3 is only found between Ambavala and Antanambe
495 (Fig. 1). The cause of potential mitonuclear discordance for *M. macarthurii* in Anjiahely was
496 subject to further investigation (see below in the section "Interspecific Gene Flow").
497

498 **Species delimitation**

499 *Genetic structure*

500 Clustering analyses (NgsAdmix and ADMIXTURE) at K = 5 grouped individuals into the
501 five nominal species in accordance with phylogenetic results and F_{ST} estimates (Fig. 4B;
502 Fig. S3; Fig. S4; Tab. S3), although some individuals were inferred to have ancestry
503 from both *M. mittermeieri* and *M. lehilahytsara* (Fig. 4B). Using NgsAdmix, three or five
504 clusters best explained the data (Fig. S3; Fig. S5), while using ADMIXTURE, three
505 clusters had a slightly lower cross-validation error than five (Fig. S5). PCA readily

506 distinguished all species (including the two sister species *M.* sp. #3 and *M. macarthurii*) across
507 the first four principal components with both GATK genotypes (Fig. 5A,B) and ANGSD
508 genotype likelihoods (Fig. S7).
509
510 When restricting clustering analyses to Clade I individuals, K = 2 was the best-supported
511 number of clusters using both approaches (Fig. S5; Fig. S6), which divided *M.*
512 *macarthurii* and *M.* sp. #3 individuals into separate clusters. At K = 3, *M.* sp. #3 split into two
513 clusters with individuals from Mananara-Nord NP and Antanambe on one hand and individuals
514 from Ambavala on the other (Fig. S8). PCA analyses for this subset of individuals clearly
515 distinguished these two groups along PC2 (Fig. 5C). Hereafter, we refer to these two groups as
516 "southern *M.* sp. #3" (Mananara-Nord NP and Antanambe are located south of the large
517 Mananara river) and "northern *M.* sp. #3" (Ambavala is located north of the river; Fig. 1).
518

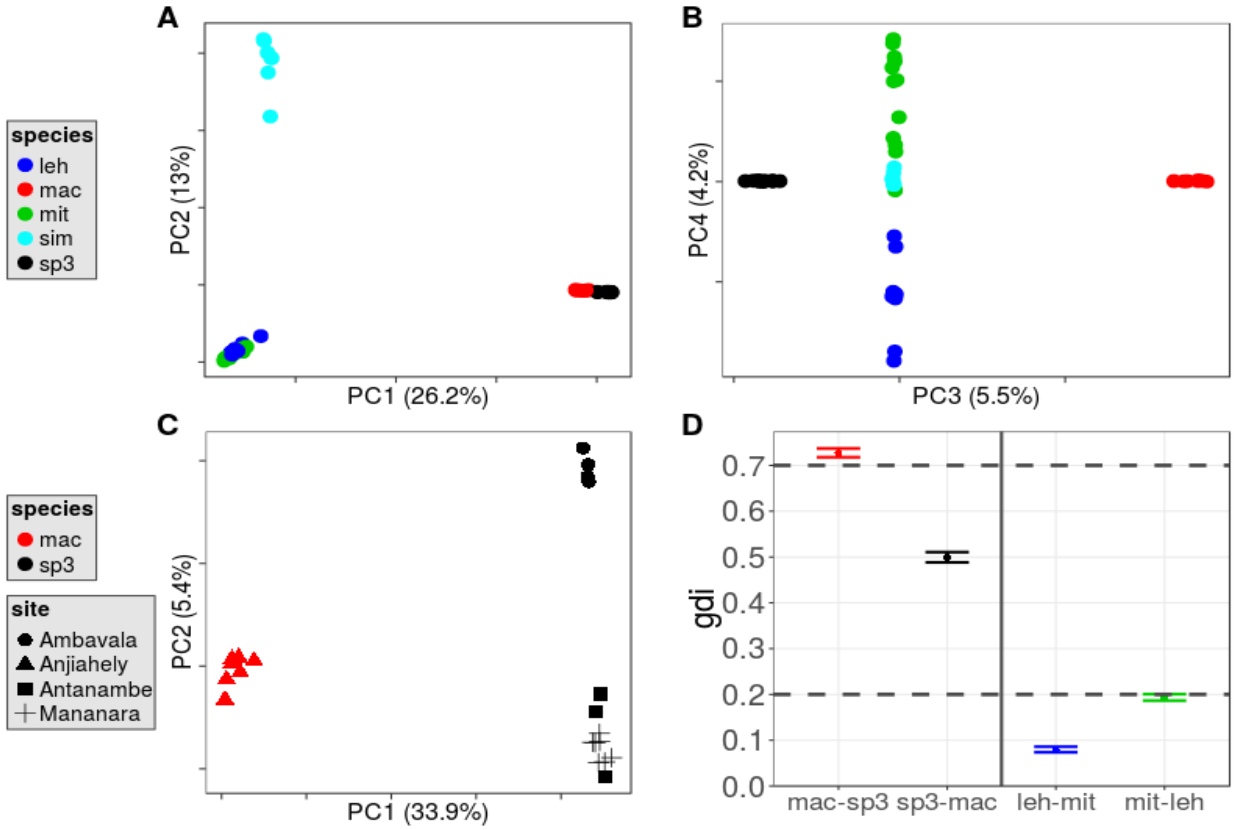

Figure 5: Population genetic structure and the *gdi*.

PCA analyses for **(A, B)** all five species and **(C)** restricted to *M*. sp. #3 and *M. macarthurii* individuals, the latter showing the split into the two population groups "northern" (Ambavala) and "southern" *M*. sp. #3 (Antanambe and Mananara-Nord NP). **(D)** Genealogical divergence index (*gdi*) for *M. macarthurii* – *M.* sp. #3 and *M. mittermeieri* – *M. lehilahytsara*. *gdi* values > 0.7 suggest separate species; *gdi* values < 0.2 are below the lower threshold for species delimitation; 0.2 < *gdi* < 0.7 are in an "ambiguous" range (Jackson et al. 2017). Abbreviations: leh: *M. lehilahytsara*, mac: *M. macarthurii*, mit: *M. mittermeieri*, sim: *M. simmonsi*, sp3: *M*. sp. #3.

SNAPP Bayes Factors

Bayes factors strongly favored splitting Clade I into two separate species in the 22-individual analyses (2lnBF = 34,326.39, Tab. 1). Bayes factors for the 22-individual dataset also supported splitting Clade II, albeit with much weaker support than Clade I (2lnBF = 993.06). All species assignments were also recovered by the guided delimitation analysis (Fig. S9).

Table 1: Bayes factor support for sister species pairs.

Marginal likelihoods were computed for a hypothesis of no speciation (Merge) and a hypothesis of a speciation event (Split). We tested the putative species pairs in both Clade I and Clade II with a 12- and 22-individual dataset. †Bayes factors calculated as 2 * ($\ln L_{Split}$ - $\ln L_{Merge}$).

Species Pair	Number of Individuals	Merge Marginal lnL	Split Marginal lnL	2ln Bayes factor†
M. macarthurii - *M. sp. #3*	12	-134254.14	-125601.69	17304.91
	22	-204540.32	-187377.12	34326.39
M. lehilahytsara - *M. mittermeieri*	12	-126515.89	-125601.69	1828.41
	22	-187873.65	-187377.12	993.06

Genealogical divergence index (gdi)

531 For the Clade I sister pair, *gdi* was 0.727 (95% HPD: 0.718-0.737) from the perspective of
532 *M. macarthurii* (i.e. above the upper threshold for species delimitation), and 0.500 (0.488-0.511)
533 from the perspective of *M*. sp. #3 (i.e. in the upper ambiguous zone for species delimitation;
534 Fig. 5D). In contrast, *gdi* values for the Clade II species pair were much lower and even below
535 the lower threshold for species delimitation: 0.080 (0.074-0.086) from the perspective of *M.*
536 *lehilahytsara*, and 0.193 (0.187-0.201) from the perspective of *M. mittermeieri* (Fig. 5D).
537
538 *Interspecific gene flow*
539 D-statistics suggested that northern *M.* sp. #3 and *M. macarthurii* with "*M. sp. #3*-type"
540 mtDNA share a slight excess of derived alleles in relation to southern *M*. sp. #3, significantly
541 deviating from 0, which indicates gene flow between northern *M*. sp. #3 and *M. macarthurii* with
542 "*M. sp. #3*-type" mtDNA (Fig. 6A). Using a G-PhoCS model with separate northern and
543 southern *M*. sp. #3 population groups, we that (1) gene flow with *M. macarthurii* took place
544 before as well as after the onset of divergence between northern and southern *M.* sp. #3, (2) gene
545 flow between extant lineages occurs only between northern (and not southern) *M.* sp. #3 and *M.*
546 *macarthurii* and (3) gene flow is asymmetric, predominantly into *M. macarthurii* (Fig. 6B). In
547 a G-PhoCS model with all species, we additionally inferred gene flow from *M. mittermeieri* to *M.*
548 *lehilahytsara* at higher levels than that from *M.* sp. #3 to *M. macarthurii* (*Fig. 7C*).
549
550 Low levels of gene flow were also inferred between the *M.* sp. #3 - *M. macarthurii* clade
551 and the *M. mittermeieri* - *M. lehilahytsara* clade, most likely between ancestral populations, but
552 the timing and direction of gene flow could not be determined in more detail (Supplementary
553 Results; Fig. S10).

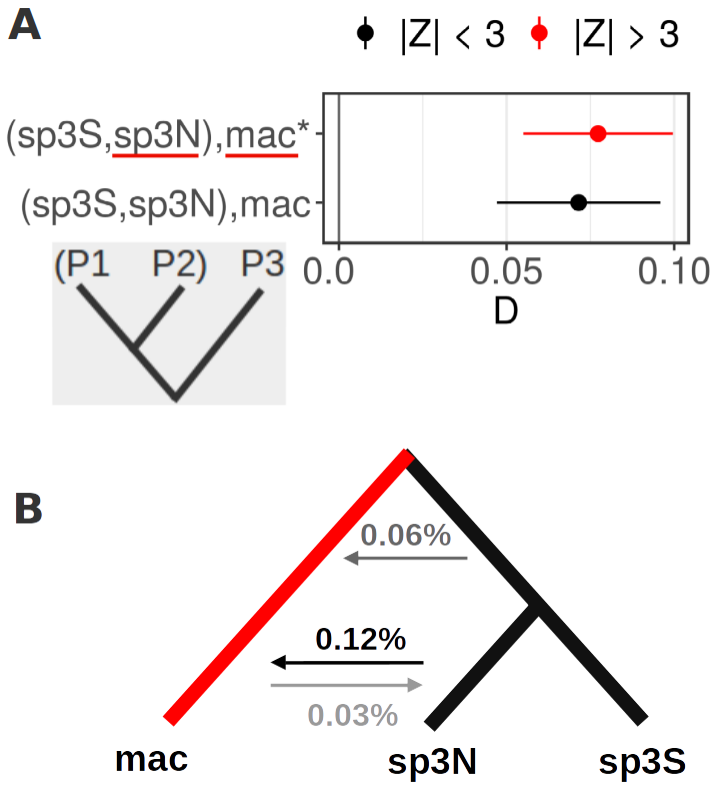

Figure 6: Gene flow between *M*. sp. #3 and *M. macarthurii*.

(A) Four-taxon D-statistics suggested gene flow between *M. macarthurii* with mitonuclear discordance ("mac*") and northern *M*. sp. #3 ("sp3N"). *M. macarthurii* with and without mitonuclear discordance ("mac") were tested separately. Axis annotations denote "(P1, P2),P3", wherein gene flow is tested between P3 and either P1 (negative D) or P2 (positive D). Significant comparisons (|Z| > 3) are in red. **(B)** Percentage of migrants in each generation, inferred by G-PhoCS under a model with three taxa: *M. macarthurii* sister taxon to northern and southern *M*. sp. #3. Different shades of gray of arrows illustrate the varying amount of gene flow.

Divergence Times

We estimated divergence times using the MSC model with BPP as well as G-PhoCS with and without interspecific gene flow (`Fig. 7; Fig. S11`). Results were similar across these approaches, although divergence times were estimated to be older in G-PhoCS models with

568 migration compared to models without migration (Fig. 7). Specifically, the divergence time of
569 Clade I was estimated at 50-109 ka (min. max. of 95% HPD across all models) without migration
570 (Fig. 7; Fig. S11), but at 91-183 ka when incorporating gene flow between the two
571 (Fig. 7). Conversely, the effect of accounting for gene flow has particularly strong effects for
572 divergence times for Clade II between *M. mittermeieri* and *M. lehilahytsara* (Fig. 7). While
573 the estimated divergence time of *M. mittermeieri* and *M. lehilahytsara* without gene flow was
574 highly similar to that between *M.* sp. #3 and *M. macarthurii* (50-97 ka; Fig. 7), it was
575 estimated to be 250-478 ka in the presence of migration (Fig. 7). Interestingly, this
576 discrepancy in age estimates under gene flow is specific two Clade II as other nodes were not
577 affected strongly by including migration into the MSC model. For example, the divergence of the
578 last common ancestor of our five focal lineages was estimated to be 351-756 ka when not
579 accounting for gene flow, and 348-648 ka when accounting for gene flow (Fig. 7D). These
580 posterior estimates are likely not influenced strongly by the model priors based on comparison of
581 marginal priors and posteriors across four BPP chains (Fig. S12).

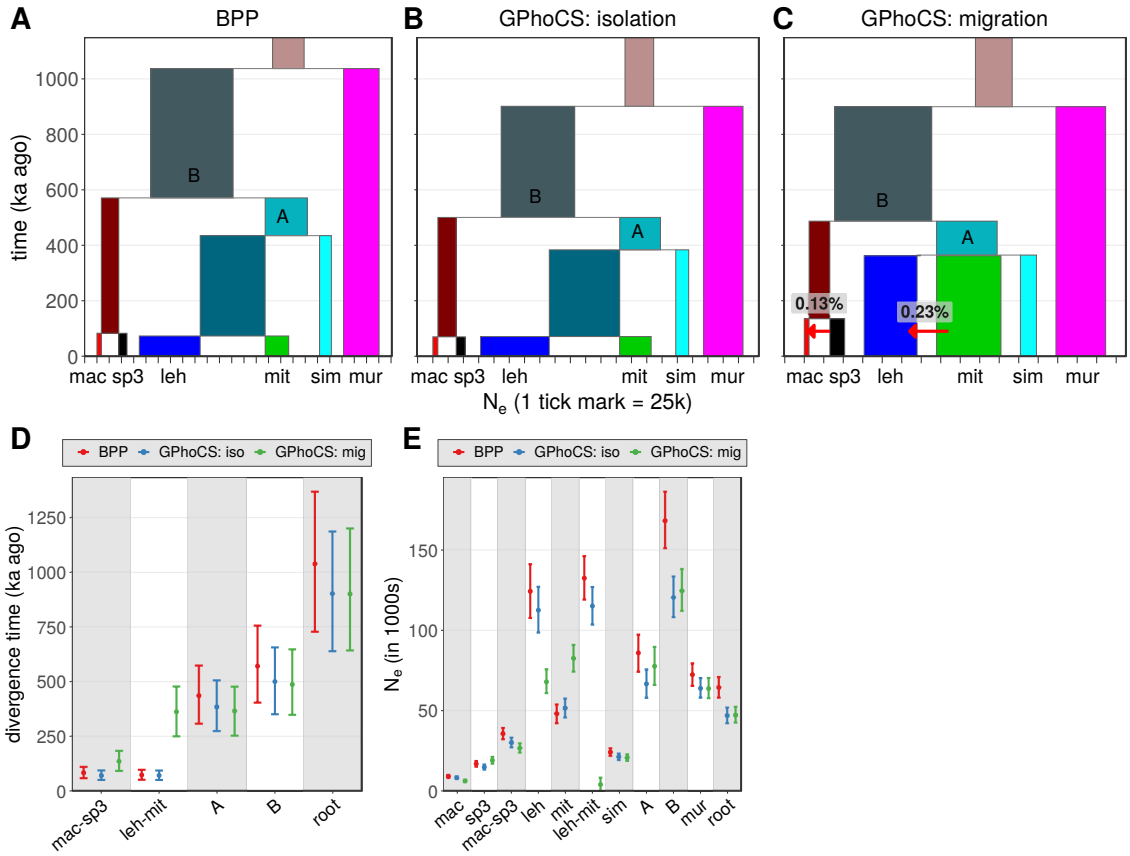

Figure 7: Demographic histories inferred by G-PhoCS and BPP.
(A-C) Divergence times (y-axis) and effective population sizes (x-axis) inferred with and without migration. **(D, E)** Comparison of divergence times and effective population sizes for each node and lineage, respectively. "A" represents the lineage ancestral to *M. simmonsi*, *M. mittermeieri* and *M. lehilahytsara*, "B" represents the lineage ancestral to *M. sp.* #3, *M. macarthurii*, *M. simmonsi*, *M. mittermeieri* and *M. lehilahytsara*, and "root" represents the lineage ancestral to all six species included.

Population sizes through time

Effective population sizes for extant as well as ancestral lineages were first estimated using BPP and G-PhoCS (with and without interspecific gene flow; `Fig. 7A-C`). We found large differences among species, with considerably larger effective population sizes for *M. murinus* (min. and max. 95% HPD across the BPP and both G-PhoCS models: 59-79 k), *M. lehilahytsara* (63-139 k), *M. mittermeieri* (42-86 k), and most ancestral lineages, than for *M.* sp. #3 (14-20 k),

596 *M. macarthurii* (6-10 k), and *M. simmonsi* (19-26 k). Wide HPD intervals for *M. mittermeieri* and
597 *M. lehilahytsara* were due to differences between models that did and did not account for gene
598 flow between these two species. Using the 3-species G-PhoCS model, effective population sizes
599 were estimated separately for northern (14-41 k), southern (7-20 k), and ancestral (18-31 k) *M.*
600 sp. #3 lineages (Fig. S10).
601
602 For one individual each of *M*. sp. #3 (from the southern group) and *M.mittermeiri*, we performed
603 MSMC analyses using whole-genome data, and compared estimates of population sizes through
604 time with those from the G-PhoCS models with and without gene flow (Fig. 8). For *M*. sp. #3,
605 estimates of population sizes through time were highly similar for all analyses and showed a
606 marked long-term decline towards the present (Fig. 8A), while estimates for *M. mittermeieri*
607 were more variable across analyses but consistently did not show a decline towards the present
608 (Fig. 8B).The estimated differences in recent effective population sizes across taxa were
609 further reflected by differences in genetic diversity across populations (Fig. S13).

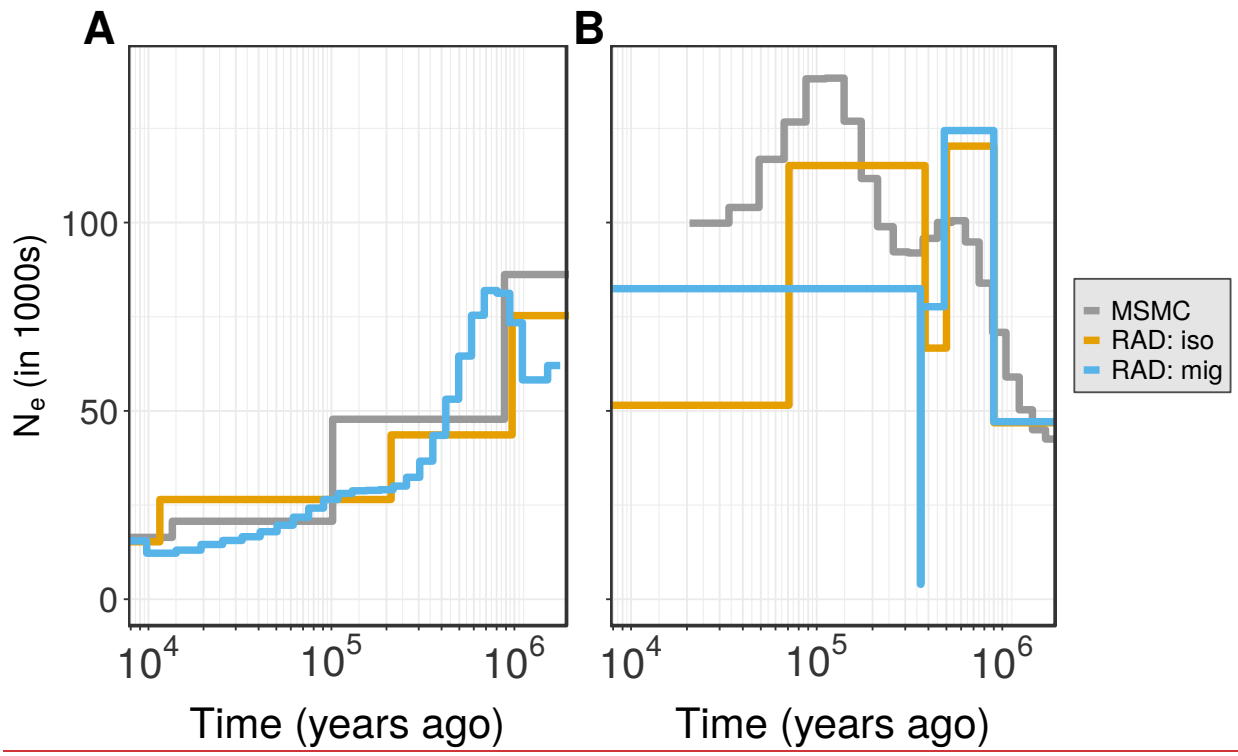

Figure 8: Estimates of effective population size through time by G-PhoCS, BPP, and MSMC. Effective population sizes through time for as inferred by MSMC for whole-genome data from a single individual (blue line), and by G-PhoCS for RADseq data without ("RAD: iso", yellow lines) and with ("RAD: mig", blue lines) gene flow. **(A)** *M*. sp. #3. G-PhoCS analyses are shown for the southern *M*. sp. #3 population group in the 3-species model, which the whole-genome individual belongs to. **(B)** *M. mittermeieri*. G-PhoCS analyses are shown for The sharp "jag" in the migration model represents a small N_e estimate for the mittermeieri-lehilahytsara ancestor, which exists for an extremely short time in this model (see Fig. 7B,C), likely preventing proper estimation of N_e.

Discussion

In this study we utilize a framework for species delimitation under complex patterns of cryptic speciation. Using this approach, we identify rapid and recent lineage diversification of mouse lemurs within a restricted region of Madagascar. Although the focal species all diverged from their common ancestors within the past 500,000 years, two pairs of non-sister species occur sympatrically. Evidence supporting the species-level divergence of *M.* sp. #3 and its sister species *M. macarthurii* (Clade I, Fig. 4) is much stronger than for the other sister species pair (Clade II, Fig. 4). Furthermore, a comparison of MSC models with and without gene flow produced substantial differences in divergence time estimates for one species pair and showed that differences in effective population size appear to have consequences for species delimitation in agreement with previous studies (Lou et al. 2018; Leaché et al. 2019).

Strong support for *M.* sp. #3 as a separate species: *M. jonahi*

Evidence for distinguishing *M.* sp. #3 as a separate species from *M. macarthurii* was strong and consistent across all applied species delimitation approaches. The two lineages were found to be reciprocally monophyletic across all phylogenetic analyses of RADseq data (Fig. 4C; Fig. S1; Fig. S2), separated unambiguously in clustering analyses (Fig. 4B; Fig. 5; Fig. S3; Fig. S5-S7), had strong support for two separate species from SNAPP Bayes factors (Tab. 1) and BPP (Fig. S9), and passed the heuristic criterion of *gdi* (Fig. 5D). Nevertheless, these two lineages have diverged from each other relatively recently, with median estimates of the divergence time across three different models with and without gene flow all under 100 ka. While recent, it is important to keep in mind that if we were to transpose the number of generations in this divergence time to a “hominin scale” (with a generation time that is seven to ten times longer than that of mouse lemurs), this would correspond to a period longer

than 500,000 years, close to the estimated divergence time between Neanderthals and *Homo sapiens*.

Though difficult to distinguish with the human eye, morphometric evidence also supported the distinctiveness of *M*. sp. #3 in comparison to all other species that occurred in the same biogeographic region (Fig. 2). *M*. sp. #3 is differentiated from its sister species *M. macarthurii* in five out of 13 measured parameters. Differences between the two sister taxa predominantly appeared in head-associated parameters such as ear and head width, orbital distances, and snout length. It has been suggested that skull parameters vary with feeding habits in lemurs and strepsirrhine primates in general (e.g., omnivorous, folivorous or frugivorous etc.; Viguier 2004; Meloro et al. 2015; Fabre et al. 2018). We hypothesize that the morphometric differences in head-associated parameters may indicate dietary and possibly cognitive differentiation between these two sister species (Zimmermann and Radespiel 2014). Based on these signatures of genomic and morphological distinctiveness, species status is supported for *M*. sp. #3 and a full species description using the name *M. jonahi* is given at the end of the manuscript.

Signatures of gene flow within a recently diverged sister species pair

Mitonuclear discordance was observed for a subset of *M. macarthurii* individuals from Anjiahely. Though having nDNA indistinguishable from other *M. macarthurii* at the same site, across phylogenetic and clustering analyses, these individuals carried mtDNA similar to that of *M.* sp. #3 (see Radespiel et al. 2008). Although genealogical discordance is not unexpected due to incomplete lineage sorting (e.g., Heckman et al. 2007; Weisrock et al. 2010), the pattern of mitochondrial introgression in phylogenetic and clustering analyses (Fig. 4) is supported by significant D-statistics between northern *M.* sp. #3 and *M. macarthurii* (Fig. 6A) and low

levels of gene flow from the northern *M.* sp. #3 population into *M. macarthurii* by G-PhoCS (Fig. 6B). This is the first case of mitochondrial introgression in mouse lemurs known to date. Therefore, the discovery of a divergent mtDNA lineage at Anjiahely (Radespiel et al. 2008; Fig. 1), which prompted the current work and has led to the discovery of a new species, appears to have been the result of a geographically localized (though incomplete) mtDNA introgression into its sister species (Clade I, Fig. 4A).

The effects of population size and gene flow for species delimitation

In contrast to *M.* sp. #3 and *M. macarthurii* (Clade I), we found only weak support for separate species status of *M. lehilahytsara* and *M. mittermeieri* (Clade II): The latter showed paraphyly in ML and SVDquartets analyses (Fig. 4A,C; Fig. S2) and were not as clearly separated in clustering analyses (Fig. 4B; Fig. S3; S5; Fig. S6). Although the Bayes factor support from SNAPP was strong by standard guidelines (Kass and Raftery 1995), the evidence was much weaker relative to species in Clade I and decreases when sampling more individuals (Tab. 1). Most strikingly, reciprocal *gdi* statistics for the lineages in Clade II were below the recommended range for diagnosing species status (Jackson et al. 2017; Leaché et al. 2019; Fig. 5D). We must therefore remain open to the possibility that boundaries between these previously described species may be ambiguous in light of new methods and results. Therefore, an important message from this study is that the methods here deployed do not necessarily lead to ever-increasing numbers of species and thus offer a reasonable way forward in our effort to accurately delimit biodiversity. Moreover, when coupled with other population genomic approaches, these methods offer insight into the complex demographic history of diverging populations, even as they are in the progressive stages of speciation.

692 Notably, some of the disparities in levels of support between the two pairs of sister species
693 may also be a direct consequence of differences in effective population sizes, which are much
694 larger for the two lineages in Clade II than for those in Clade I. This may clearly impact the *gdi*
695 which is calculated using the estimated population sizes and divergence times without accounting
696 for potential gene flow. Since those divergence time estimates are highly similar for both species
697 pairs, the difference in *gdi* must therefore largely be the result of differences in effective
698 population sizes. This is expected, since larger effective population sizes result in slower sorting
699 of ancestral polymorphisms (Maddison 1997), and the *gdi* relies on quantifying the probability
700 that two sequences from the focal taxon coalesce more recently than the divergence time between
701 the taxa. More generally, differences in N_e may also explain why *M. mittermeieri* and *M.*
702 *lehilahytsara* were not resolved as clades in the nDNA phylogeny (Fig. 4C) yet are shown to
703 have distinct genetic clusters (Fig. 4B; Fig. 5B). Thus, our empirical results mirror those
704 anticipated in a recent simulation study (Leaché et al. 2019).
705
706 Assessing speciation completion by quantifying rates of neutral coalescence is based on the
707 assumption that the magnitude of genetic drift is a good predictor of progress in speciation. This
708 is problematic, however, given that the role of drift in speciation is generally thought to be small
709 (Rice and Hostert 1993; Coyne and Orr 2004; Czekanski-Moir and Rundell 2019; but see Uyeda
710 et al. 2009), and a high prevalence of gene flow during and after speciation (Feder et al. 2012;
711 Harrison and Larson 2014; Mallet et al. 2016; Campbell et al. 2018) may restrict the build-up of
712 neutral differentiation, even over longer time spans. While the general possibility that progress in
713 speciation is decoupled from neutral genetic differentiation should be kept in mind when
714 delimiting species using molecular data (Guilot et al. 2012; Solis-Lemus et al. 2015), a reliance
715 on genealogical divergence in coalescence-based species delimitation specifically renders

716 effective population size a key variable. It is not clear whether this is justified, however,
717 indicating that additional measures of divergence that do not depend on effective population sizes
718 may also need to be considered (see also Hey and Pinho 2012; Martien et al. 2017 – Appendix 2).
719 We raise this point specifically given that only a few studies have examined a potential link
720 between N_e and speciation rates (Khatri and Goldstein 2015; Khatri and Goldstein 2018; Huang
721 et al. 2018), especially outside of the context of founder effect speciation (Mayr 1959; Boake and
722 Gavrilets 1998; Matute 2013).
723
724 A further distinction between the two pairs of sister species examined by this study is that
725 we find higher rates of gene flow between the lineages in Clade II, at 0.23%, than those in Clade
726 I, at 0.13% (Fig. 7C). This is not simply a consequence of overall lower differentiation, given
727 that divergence time estimates are considerably older in Clade II when a model with gene flow is
728 implemented. Specifically, the model incorporating gene flow between *M. lehilahytsara* and *M.*
729 *mittermeieri* shifted their divergence time backwards by nearly 300 ka, though estimates for
730 deeper nodes were not similarly affected. The substantial effect of incorporating or disregarding
731 gene flow on divergence time estimation has been previously noted (Leaché et al. 2014) and we
732 here reiterate its importance for future studies. Thus, a joint consideration of genealogical
733 divergence and rates of gene flow may offer a way forward for effective and consistent genomic
734 species delimitation (see also Hey and Pinho 2012) with our study showing that this is an area
735 ripe for future exploration.
736
737 **Rapid speciation in mouse lemurs**
738 Sympatric *Microcebus* species were found at two study sites, with representatives of both
739 Clade I (*M. macarthurii*) and Clade II (*M. mittermeieri*) in Anjiahely (Makira) as well as in

740 Ambavala (*M*. sp. #3 and *M. lehilahytsara* - Clades I and II, respectively; Fig. 1). This is
741 remarkable given that only four other cases of sympatry among mouse lemur species are known,
742 always with *M. murinus* as the co-resident (Radespiel 2016). Given that Clades I and II are
743 estimated to have a common ancestor as recently as ~500-600 ka, this provides compelling
744 evidence that mouse lemurs not only developed widespread and rapid genetic divergence among
745 geographic areas, but also rapid reproductive isolation. Assuming that the geographic mode of
746 speciation has been largely allopatric, the observed sympatry of two pairs of non-sister species
747 also reveals substantial range dynamics of at least some of the focal species. It is tempting to
748 speculate that secondary contact occurred due to range expansion of *M. mittermeieri* and *M.*
749 *lehilahytsara* (Clade II), which have larger ranges and population sizes as well as higher levels of
750 interspecific gene flow than the decreasing micro-endemics *M.* sp. #3 and *M. macarthurii* (Clade
751 I).
752
753 Coalescent-based estimates of divergence times constrain the speciation of the focal
754 lineages to the Pleistocene (<600,000 years). It is therefore plausible that past climatic
755 oscillations, especially periods of drought accompanied with turnovers in vegetation composition
756 and the contraction of forested habitats were a factor in the isolation and genetic divergence of
757 the sampled species and populations (Burney et al. 1997; Gasse and Van Campo 2001; Kiage and
758 Liu 2006; Wilmé et al. 2006). In addition, the Mananara river appears to have impacted
759 population structure within *M*. sp. #3 and restricted gene flow between *M*. sp. #3 south of the
760 Mananara river and *M. macarthurii*, further emphasizing that large rivers can be phylogeographic
761 barriers in lemurs (Martin 1972; Pastorini et al. 2003; Goodman and Ganzhorn 2004; Olivieri et
762 al. 2007).
763

764 A notable feature of the coalescent-based estimates of divergence times presented here is
765 that they are drastically different compared to those derived from fossil-calibrated molecular
766 clock methods. The basal divergence between *M. murinus* and the focal five-species clade in this
767 study was estimated to be close to 1 ma with MSC methods but has previously been estimated to
768 be approximately 8 - 10 ma using fossil-calibrated estimates (Yang and Yoder 2003; dos Reis et
769 al. 2018). Several factors may explain this difference: First, we used a recent pedigree-based
770 estimate of the mouse lemur mutation rate that is about 2.5-fold higher than the phylogenetically-
771 based estimate for mouse lemurs (Campbell et al. 2019). Second, concatenated and gene tree-
772 based estimates are theoretically expected to overestimate recent species divergence times
773 (Edwards and Beerli 2000; Arbogast et al. 2002) and empirical comparisons have indeed found
774 considerably more recent divergence time estimates using coalescent-based estimates
775 (McCormack et al. 2011; Angelis & Dos Reis 2015; Colombo et al. 2015). Finally, fossil-
776 calibrated estimates for lemurs require external calibrations from distantly related lineages given
777 the absolute dearth of lemur fossils (e.g., Yang and Yoder 2003; Herrera and Dávalos 2016). In
778 summary, the mouse lemur radiation is likely more recent than previously suggested, yet further
779 investigation is needed to understand the magnitude of these disparate estimates.
780

781 **Endangered "hotspot for micro-endemism" in northeastern Madagascar and other**
782 **geographic considerations**

783 In total, we found five evolutionarily divergent lineages of *Microcebus* within a 130 km
784 wide stretch of lowland rain forest in northeastern Madagascar making this restricted region one
785 of the most biodiverse areas thus far identified for mouse lemurs. Although all taxa can be found
786 in varying habitat types (except heavily degraded grass- and fernlands), primary forests, even of

787 varying degradation stages, are preferred (Knoop et al. 2018; Miller et al. 2018; Schüßler et al.
788 2018).
789
790 A long-term decline in population size was inferred for the lineage leading to *M*. sp. #3.
791 While changes in inferred N_e may be confounded by changes in population structure, especially
792 for single-population PSMC/MSMC models that do not explicitly consider population
793 subdivision (Mazet et al. 2016; Chikhi et al. 2018), we found highly congruent results between
794 MSMC and G-PhoCS analyses that considered divergence across a model with three species,
795 treating the two *M.* sp. #3 population clusters separately (Fig. 7F). This is especially
796 supportive given that although the MSMC analysis used whole-genome data for only a single
797 individual, RADseq data from multiple individuals per population underly the G-PhoCS
798 analyses. Importantly, changes in population structure may also be associated with actual changes
799 in population size, such as successive population subdivision events with limited or no
800 subsequent gene flow. If such changes in population structure are the primary cause of population
801 size changes, as appears to be the case for the lineage leading to *M.* sp. #3, a high degree of
802 concordance between these different types of analyses would in fact be expected. Nevertheless,
803 we stress that future work should focus on more complex scenarios of connectivity using
804 metapopulation models, as has been suggested for humans (Scerri et al. 2018).
805
806 Relevant to human impacts and the natural history of Madagascar, the decline and
807 population subdivision of *M*. sp. #3 was clearly inferred to have started long before
808 anthropogenic land use fragmented the forest habitats, supporting the emerging consensus that
809 human colonization in Madagascar alone does not explain the occurrence of open habitats and
810 isolated forest fragments (Quéméré et al. 2012; Vorontsova et al. 2016; Yoder et al. 2016; Hackel

et al. 2018). However, we also observed clade-specific population size dynamics within the same region, with the lineages in Clade II maintaining much larger population sizes than those in Clade I. This may be explained by differences in altitudinal range between the two clades: whereas *M.* sp. #3 and *M. macarthurii* appear to occur only in lowland forests, *M. lehilahytsara* and *M. mittermeieri* occur at both higher and lower elevations, perhaps providing population connectivity under a scenario in which rivers act differentially as barriers for gene flow as has been suggested by Wilmé et al. (2006) .

The results of our study emphasize the need to intensify conservation activities in this region (Schüßler et al. 2018). The exact range of *M.* sp. #3 is not yet established, but likely does not exceed a maximum size of about 4,500 km². The known distribution includes community-protected forests around Ambavala (Schüßler et al. 2018) and one nationally protected area within Mananara-Nord NP. The southern range boundary of this species is most likely the Anove river (Fig. 1), given that we detected *M. simmonsi* directly south of this river (which represents a northern expansion of the known range for *M. simmonsi* that had previously been found at Zahamena NP, Betampona and Tampolo; Louis et al. 2006; Louis and Lei 2016).

Although *M. lehilahytsara* has been assumed to represent a highland specialist, with no previous records below 825 m a.s.l. (Weisrock et al. 2010; Radespiel et al. 2012), individuals at Ambavala, at an elevation of 235 m a.s.l. are placed in the same clade as *M. lehilahytsara* from a highland study site (Riamalandy). This finding needs to be interpreted with caution, however, due to weak overall differentiation between *M. lehilahytsara* and *M. mittermeieri* and a lack of samples from intermediate locations. Thus, further research is required to resolve this relationship and implications for the evolutionary history and biogeography of *M. lehilahytsara*.

835

836 Recent analyses show that preferred forest habitats are rapidly declining, and the isolation
837 of protected areas appears to be inevitable (Schüßler et al. in revision). We are now beginning to
838 appreciate that the area of northeastern Madagascar also represents a hotspot for micro-
839 endemism, with a newly described species already facing high extinction risk due to ongoing
840 deforestation (Schüßler et al. in revision) and anticipated environmental disruptions due to
841 climate change (Brown and Yoder 2015). This situation is unfortunately reminiscent of the recent
842 discovery of the Tapanuli orangutan (*Pongo tapanuliensis*), which became the last great ape
843 species to be discovered and the most threatened at the same time (Nater et al. 2017).

844

845 **Conclusions**

846 The results of this study have verified divergent evolution and reproductive isolation in
847 primate species that are virtually indistinguishable to human eyes thus emphasizing the relevance
848 of the multispecies coalescent for investigating the forces that drive speciation in radiations of
849 cryptic species. We find that careful consideration is required when variation in N_e among
850 lineages is high. As has been predicted by simulation studies, we observed that lineages with high
851 N_e did not pass the *gdi* criterion for species delimitation (Leaché et al. 2019). These same
852 lineages were paraphyletic in standard phylogenetic analyses, though Bayes factor delimitation
853 approaches would consider them separate species. Confounding effects of gene flow when
854 estimating divergence times were also revealed when comparing MSC analyses that did or did
855 not consider migration, and we anticipate that this is an area ripe for further exploration in other
856 biological systems.

857

858 Though of limited phylogenetic breadth, the results of this study have touched on issues of
859 broad relevance for investigating the forces that drive rapid speciation in radiations of cryptic
860 species. Though we find that this radiation of cryptic primates has occurred quite recently in
861 geological time, when one considers that divergence ages are here calculated in coalescent units,
862 which are scaled with generation time, it is not surprising that the short generation times
863 characteristic of mouse lemurs may predispose them to respond rapidly to changing
864 environmental circumstances. Given that Madagascar experienced dramatic vegetative changes
865 coinciding with climactic oscillations through the Pleistocene, our finds are consistent with the
866 hypothesis that patterns of explosive lineage diversification in the mouse lemur clade may have
867 been driven by rapid environmental change.

Species Description

Systematics

Order: Primates (Linnaeus 1758)

Suborder: Strepshirrini (É. Geoffroy 1812)

Family: Cheirogaleidae (Gray 1873)

Genus: *Microcebus* (É. Geoffrroy 1828)

Species: *Microcebus jonahi* species nova

Holotype

B34, adult male, captured on 06 September 2017 by DS. Tissue samples, hair samples as well as e-voucher photos of the animal are stored at the Institute of Zoology, University of Veterinary Medicine Hanover, Germany. The animal itself was released after field handling, sampling, and photographing, since its taxonomic distinctiveness was not recognized at the time of capture. Field measurements (all lengths measured in mm): ear length: 17.6, ear width: 13.7, head length: 37.7, head width: 23.0, snout length: 10.0, intra-orbital distance: 8.2, inter-orbital distance: 26.0, lower leg length: 41.7, hind foot length: 24.5, third toe length: 10.6, body length: 95.6, tail length: 130.0, body mass: 66 g. The population around Ambavala is designated as the source population for physical specimens in support of the holotype.

Type locality

Forest near the rural village of Ambavala (S 16° 12.307’, E 49° 35.371’), in a community protected forest at about 342 m a.s.l. approx. 20 km west of Mananara North, Province of Analanjirofo, Madagascar.

Paratypes

(a) BD1, adult female, captured in the community protected forest of Antsiradrano (near Ambavala) on 04 September 2017. Tissue and hair samples as well as photographs and morphometric measurements are stored at the Institute of Zoology, University of Veterinary Medicine Hanover, Germany.

(b) B13, adult male, captured in the community protected forest near Ambavala on 11 September 2017. Tissue and hair samples as well as photographs and morphometric measurements are stored at the Institute of Zoology of the University of Veterinary Medicine Hanover in Germany.

It is planned that one physical specimen will be obtained as a further paratype in the near future and that this specimen will then be deposited in the Museum of the Zoology, Department of the University of Antananarivo, Madagascar.

Description

Microcebus jonahi is a large-bodied, reddish-brown and small-eared mouse lemur (Fig. 9). This species has short and dense fur. The head is rufous colored with a darker brownish area around the eyes which can slightly vary among individuals. A distinct white stripe lies between the eyes ending at the forehead (Fig. 9C). The ears are of the same rufous color as the head. The cheeks are lighter brownish and less rufous than the head becoming even lighter and almost white towards the throat. The ventrum is white with slightly yellowish nuances (Fig. 9D) which can vary in appearance among individuals. The dorsum is rather uniformly brown than reddish (Fig. 9E). A darker dorsal stripe can be either present or absent. The ventrum and dorsum are separated by a significant change in coloration with only marginal transition. The coloration of the limbs shows the same pattern with a brownish dorsal and a white to slightly

yellowish ventral side. The tail is densely furred and of the same coloration as the dorsum. Hands and feet show only sparse but whitish-gray hair. The skin on the palmar and plantar surfaces of hands and feet is brownish-pink. Males and females do not show any sexual dimorphism.

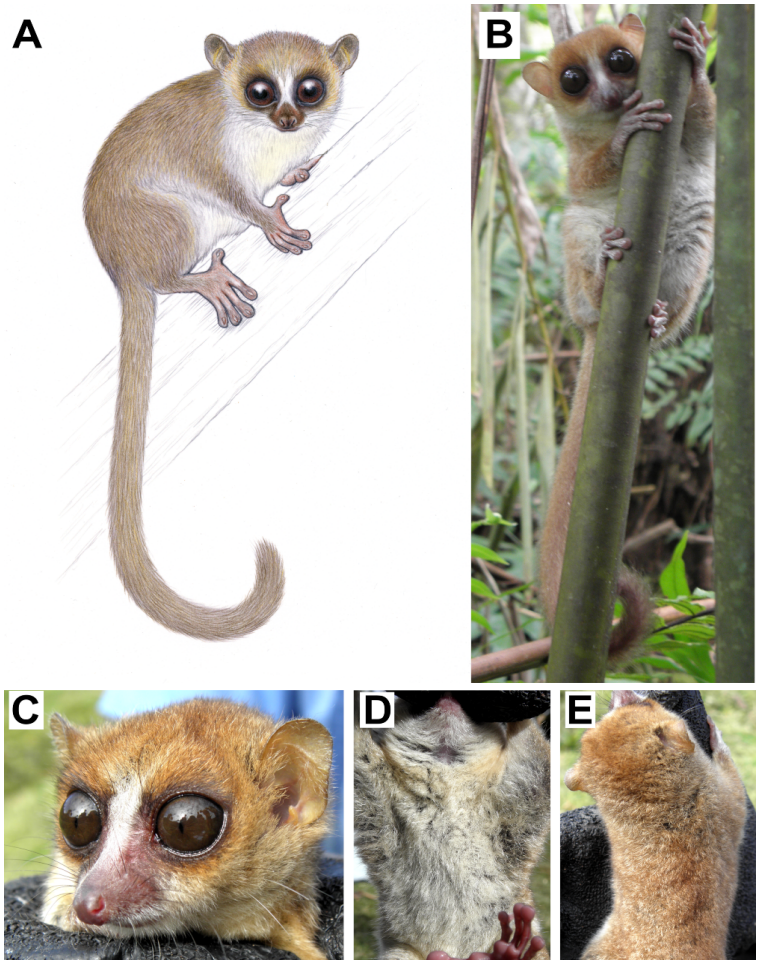

Figure 9: Outer morphology of *Microcebus jonahi*. (A) Drawing of an adult individual; (B) Habitus of adult female (paratype individual BD1); (C-E) Close-ups of adult male (holotype B34). Illustration copyright by Stephen D. Nash / IUCN SSC Primate Specialist Group; used with permission. Photos by D. Schüßler.

Diagnosis

M. jonahi can be distinguished from other taxa in northeastern Madagascar by morphometric and genetic differences. Compared to its closest relative, *M. macarthurii*, *M. jonahi* has a larger snout

length, ear and head width as well as a larger intra- and inter-orbital distance. In addition, *M. jonahi* can be easily differentiated from *M. macarthurii* by its ventral coloration which is rather whitish (*Fig. 9*), but distinctly yellowish-orange in *M. macarthurii* (Radespiel et al. 2008; Radespiel and Raveloson unpubl. data).

Moreover, it can be easily distinguished from the sympatric, small-bodied *M. lehilahytsara* (at Ambavala) by its higher weight, larger body size and tail length. Finally, *M. jonahi* can be differentiated from its southern geographical neighbor, *M. simmonsi*, by its larger head width as well as wider inter- and intra-orbital distances. *M. jonahi* could be unambiguously distinguished from the other four taxa in this study across all analyses of nuclear RADseq data (see above). However, it may not be reliably distinguished from *M. macarthurii* based solely on mtDNA sequences, likely due to some introgression of mtDNA from *M. jonahi* into *M. macarthurii* (see above) in the past.

Etymology

M. jonahi is named in honor of Malagasy primatologist Professor Jonah Ratsimbazafy. He has dedicated his life's work to the conservation of Malagasy lemurs. With both national and international outreach to the scientific community (e.g., GERP, IPS, LemurPortal), to the public of Madagascar (e.g., by initiating the World Lemur Festival), and to the political leaders of Madagascar, he serves as an inspirational role model for young Malagasy students and scientists. He provides hope for the future of Madagascar and for its iconic lemurs during very challenging times.

Vernacular name

English name: Jonah's mouse lemur, French name: Microcèbe de Jonah, German

name: Jonah’s Mausmaki.

Acknowledgements

This study was conducted under the research permit No. 197/17/MEEF/SG/DGF/DSAP/SCB.Re (DS), 072/15/MEEMF/SG/DGF/DCB.SAP/SCB (MBB), 137/13/MEF/SG/DGF/DCB.SAP/SCB (DWR), 175/14/MEF/SG/DGF/DCB.SAP/SCB (AM), kindly issued by the directeur du système des aires protégées, Antananarivo and the regional authorities (Direction Régional de l'Environnement, de l'Ecologie et de Forêts). We are endebted to J.H. Ratsimbazafy, N.V. Andriaholinirina, C. Misandeau, B. Le Pors and S. Rasoloharijaona, for their help with administrative tasks and to G. Besnard for facilitating this study. We thank our field assistants (I. Sitrakarivo, C. Hanitriniaina and T. Ralantoharijaona) and the ADAFAM (Association Des Amis de la Forêt d'Ambodiriana-Manompana) for their valuable help during sample collection. We warmly thank the many local guides and cooks for sharing their incomparable expertise and help in the field, *misaotra anareo jiaby*.

Funding was granted by the Bauer Foundation and the Zempelin Foundation of the "Deutsches Stiftungszentrum" under grant no. T237/22985/2012/kg and T0214/32083/2018/sm to DS, Duke Tropical Conservation Initiative Grant to ADY, and Duke Lemur Center/SAVA Conservation research funds to MBB, the School of Animal Biology at The University of Western Australia to AM, the Fundação para a Ciência e a Tecnologia, Portugal (PTDC/BIA-BEC/100176/2008, PTDC/BIA-BIC/4476/2012, and SFRH/BD/64875/2009), the Groupement de Recherche International (GDRI) Biodiversité et développement durable – Madagascar, the Laboratoire d'Excellence (LABEX) TULIP (ANR-10-LABX-41) and CEBA (ANR-10-LABX-25-01, the Instituto Gulbenkian de Ciência, Portugal to LC and JS, the ERA-NET BiodivERsA project: INFRAGECO (Inference, Fragmentation, Genomics, and Conservation, ANR-16-EBI3-0014 & FCT-Biodiversa/0003/2015) the LIA BEEG-B (Laboratoire International Associé –

975 Bioinformatics, Ecology, Evolution, Genomics and Behaviour, CNRS) to LC and JS. Further
976 financial support came from the Institute of Zoology, University of Veterinary Medicine
977 Hannover and UR acknowledges the long-term support of the late Elke Zimmermann for her
978 research activities on Madagascar. The genomic data were generated with funds from NSF DEB-
979 1354610 to ADY and DWW and from the EDB Lab to JS. ADY also gratefully acknowledges
980 support from the John Simon Guggenheim Memorial Foundation and the Alexander von
981 Humboldt Foundation. EELJ would like to acknowledge support from the Ahmanson Foundation
982 for the data generation. This work was performed in collaboration with the GeT core facility,
983 Toulouse, France (http://get.genotoul.fr), and was supported by France Génomique National
984 infrastructure, funded as part of "Investissement d'avenir" program managed by Agence
985 Nationale pour la Recherche (contract ANR-10-INBS-09). JS, UR & LC also gratefully
986 acknowledge support from the Get-Plage sequencing and Genotoul bioinformatics
987 (BioinfoGenotoul) platforms Toulouse Midi-Pyrenees.

988 **References**

989 Adams M., Raadik T.A., Burridge C.P., Georges A. 2014. Global biodiversity assessment and
990 hyper-cryptic species complexes: more than one species of elephant in the room? *Syst. Biol.*
991 63:518-533.

992 Alexander D.H., Novembre J., Lange K. 2009. Fast model-based estimation of ancestry in
993 unrelated individuals. *Genome Res.* 19:1655–1664.

994 Ali O. A., O'Rourke S. M., Amish S. J., Meek M. H., Luikart G., Jeffres C., Miller M. R. 2016.
995 RAD capture (rapture): Flexible and efficient sequence-based genotyping. *Genetics*
996 202:389–400.

997 Angelis K., Dos Reis M. 2015. The impact of ancestral population size and incomplete lineage
998 sorting on Bayesian estimation of species divergence times. *Cur. Zool.* 61:874-885.

999 Barley A. J., Brown J. M., Thomson R. C. 2017. Impact of model violations on the inference of
1000 species boundaries under the multispecies coalescent. *Syst. Biol.* 67:269–284.

1001 Beaumont M. A. 2004. Recent developments in genetic data analysis: What can they tell us about
1002 human demographic history? *Heredity* 92:365–379.

1003 Boetzer M., Henkel C. V., Jansen H. J., Butler D., Pirovano W. 2011. Scaffolding pre-assembled
1004 contigs using sspace. *Bioinformatics* 27:578–579.

1005 Brown J. L., Yoder A. D. 2015. Shifting ranges and conservation challenges for lemurs in the face
1006 of climate change. *Ecol. Evol.* 5:1131–1142.

1007 Bryant D., Bouckaert R., Felsenstein J., Rosenberg N. A., RoyChoudhury A. 2012. Inferring
1008 species trees directly from biallelic genetic markers: bypassing gene trees in a full coalescent
1009 analysis. *Mol. Biol. Evol.* 29:1917–1932.

1010 Burney D., James H., Grady F., Rafamantanantsoa J. G., Wright H., Cowart J. 1997.
1011 Environmental change, extinction and human activity: evidence from caves in NW
1012 Madagascar. *J. Biogeogr.* 24:755–767.
1013 Campbell C. R., Poelstra J. W., Yoder A. D. 2018. What is speciation genomics? The roles of
1014 ecology, gene flow, and genomic architecture in the formation of species. *Biol. J. Linn. Soc.*
1015 124:561–583.
1016 Campbell C. R., Tiley G. P., Poelstra J. W., Hunnicutt K. E., Larsen P. E., dos Reis M., Yoder A.
1017 D. 2019. Pedigree-based measurement of the de novo mutation rate in the gray mouse lemur
1018 reveals a high mutation rate, few mutations in CpG sites, and a weak sex bias. BiorXiv,
1019 posted August 5, 2019. doi: https://doi.org/10.1101/724880.
1020 Carstens BC, Dewey TA. 2010. Species delimitation using a combined coalescent and
1021 information-theoretic approach: An example from North American *Myotis* bats. Syst Biol.
1022 59:400-414.
1023 Chambers E. A., Hillis D. M. 2019. The multispecies coalescent over-splits species in the case of
1024 geographically widespread taxa. *Syst. Biol.* 68:doi: org/10.1093/sysbio/syz042.
1025 Chifman J., Kubatko, L. 2014. Quartet inference from SNP data under the coalescent model.
1026 *Bioinformatics* 30:3317–3324.
1027 Chikhi L., Sousa V., Luisi P., Goossens B., Beaumont M.A. 2010. The confounding effects of
1028 population structure, genetic diversity and the sampling scheme on the detection and
1029 quantification of population size changes. *Genetics* 186:983-995.
1030 Chikhi L., Rodríguez W., Grusea S., Santos P., Boitard S., Mazet O. 2018. The IICR (inverse
1031 instantaneous coalescence rate) as a summary of genomic diversity: insights into
1032 demographic inference and model choice. *Heredity* 120:13-24.

1033 Colombo M., Damerau M., Hanel R., Salzburger W., Matschiner M. 2015. Diversity and disparity
1034 through time in the adaptive radiation of Antarctic notothenioid fishes. *J. Evol. Biol.* 28:376–
1035 394.
1036 Coyne J., Orr H. 2004. *Speciation*. Sinauer Associates, Sunderland.
1037 Czekanski-Moir J. E., Rundell R. J. 2019. The ecology of nonecological speciation and
1038 nonadaptive radiations. *Trends Ecol. Evol.* 34:400–415.
1039 Dalquen D. A., Zhu T., Yang Z. 2017. Maximum likelihood implementation of an isolation-with-
1040 migration model for three species. *Syst. Biol.*66:379-398.
1041 Dávalos L. M., Russell A. L. 2014. Sex-biased dispersal produces high error rates in
1042 mitochondrial distance-based and tree-based species delimitation. *J. Mammal.*95:781–791.
1043 Degnan J.H., Rosenberg N.A. 2006. Discordance of species trees with their most likely gene
1044 trees. *PLoS Genet*. 2:e68.
1045 De Queiroz K. 2007. Species concepts and species delimitation. *Syst. Biol.*56:879–886.
1046 DePristo M. A., Banks E., Poplin R., Garimella K. V., Maguire J. R., Hartl C., Philippakis A. A.,
1047 Del Angel G., Rivas M. A., Hanna M., McKenna A., Fennell T. J., Kernytsky A. M.,
1048 Sivachenko A. Y., Cibulskis K., Gabriel S. B., Altshuler D., Daly M. J. 2011. A framework
1049 for variation discovery and genotyping using next-generation DNA sequencing data. *Nat.*
1050 *Genet.* 43:491–498.
1051 Displayr. 2018. flipMultivariates R package. URL https://github.com/Displayr/flipMultivariates
1052 Dos Reis M., Gunnell G. F., Barba-Montoya J., Wilkins A., Yang Z., Yoder A. D. 2018. Using
1053 phylogenomic data to explore the effects of relaxed clocks and calibration strategies on
1054 divergence time estimation: Primates as a test case. *Syst. Biol.*67:594–615.
1055 Edwards D. L., Knowles L. L. 2014. Species detection and individual assignment in species
1056 delimitation: can integrative data increase efficacy? *Proc. Roy. Soc. B* 281:20132765.

1057 Edwards S. V., Beerli P. 2000. Gene divergence, population divergence, and the variance in
1058 coalescent time in phylogeographic studies. *Evolution* 54:1839–1854.
1059 Eriksson A., Manica A. 2012. Effect of ancient population structure on the degree of
1060 polymorphism shared between modern human populations and ancient hominins. *Proc. Natl.*
1061 *Acad. Sci. USA* 109:13956-13960.
1062 Estrada A., Garber P. A., Rylands A. B., Roos C., Fernandez-Duque E., Di Fiore A., Nekaris
1063 K. A. I., Nijman V., Heymann E. W., Lambert J. E., Rovero F., Barelli C., Setchell J. M.,
1064 Gillespie T. R., Mittermeier R. A., Arregoitia L. V., de Guinea M., Gouveia S., Dobrovolski
1065 R., Shanee S., Shanee N., Boyle S. A., Fuentes A., MacKinnon K. C., Amato K. R., Meyer
1066 A. L. S., Wich S., Sussman R. W., Pan R., Kone I., Li B. 2017. Impending extinction crisis of
1067 the worlds primates: Why primates matter. *Sci. Adv.* 3:e1600946.
1068 Fabre A. C., Perry J. M., Hartstone-Rose A., Lowie A., Boens A., Dumont M. 2018. Do muscles
1069 constrain skull shape evolution in strepsirrhines? *Anat. Rec.* 301:291–310.
1070 Feder J. L., Egan S. P., Nosil P. 2012. The genomics of speciation-with-gene-flow. *Trends Genet.*
1071 28:342–350.
1072 Fiser C., Robinson C.T., Malard F. 2018. Cryptic species as a window into the paradigm shift of
1073 the species concept. *Mol. Ecol.* 27:613-635.
1074 Flouri T., Jiao, X., Rannala B., Yang Z. 2018. Species tree inference with BPP using genomic
1075 sequences and the multispecies coalescent. *Mol. Biol. Evol.* 35:2585–2593.
1076 Fox J. and Weisberg S. 2011. An R Companion to Applied Regression. Second Edition. Sage,
1077 Thousand Oaks CA. URL http://socserv.socsci.mcmaster.ca/jfox/Books/Companion
1078 Fujita M.K., Leache A.D., Burbrink F.T., McGuire J.A., Moritz C. 2012. Coalescent-based
1079 species delimitation in an integrative taxonomy. *Trends Ecol. Evol.* 27:480-488.

1080 Fumagalli M., Vieira F. G., Korneliussen T. S., Linderoth T., Huerta-Sánchez E., Albrechtsen A.,
1081 Nielsen R. 2013. Quantifying population genetic differentiation from next-generation
1082 sequencing data. *Genetics* 195:979-992.
1083 Fumagalli M., Vieira F. G., Linderoth T., Nielsen R. 2014. ngstools: methods for population
1084 genetics analyses from next-generation sequencing data. *Bioinformatics* 30:1486–1487.
1085 Gasse F., Van Campo E. 2001. Late quaternary environmental changes from a pollen and diatom
1086 record in the southern tropics (lake Tritrivakely, Madagascar). *Palaeogeogr. Palaeoclimatol.*
1087 *Palaeoecol.* 167:287–308.
1088 Gavrilets, S. Boake C. R. 1998. On the evolution of premating isolation after a founder event.
1089 *Am. Nat.* 152:706–716.
1090 Gonen S., Bishop S. C., Houston R. D. 2015. Exploring the utility of cross-laboratory rad-
1091 sequencing datasets for phylogenetic analysis. *BMC Res. Notes* 8:299.
1092 Goodman S. M., Benstead J. P. 2005. Updated estimates of biotic diversity and endemism for
1093 Madagascar. *Oryx* 39:73–77.
1094 Goodman S. M., Ganzhorn J. U. 2004. Biogeography of lemurs in the humid forests of
1095 Madagascar: the role of elevational distribution and rivers. *J. Biogeogr.* 31:47–55.
1096 Goudet J. 2005. Hierfstat, a package for R to compute and test hierarchical f-statistics. *Mol. Ecol.*
1097 *Notes* 5:184–186.
1098 Gronau I., Hubisz M. J., Gulko B., Danko C. G., Siepel A. 2011. Bayesian inference of ancient
1099 human demography from individual genome sequences. *Nat. Genet.* 43:1031–1034.
1100 Grummer JA, Bryson RW Jr, Reeder TW. 2013. Species delimitation using Bayes factors:
1101 simulations and application to the Sceloporus scalaris species group (Squamata:
1102 Phrynosomatidae). Syst. Biol. 63:119-133.

1103 Hackel J., Vorontsova M. S., Nanjarisoa O. P., Hall R. C., Razanatsoa J., Malakasi P., Besnard G.
1104 2018. Grass diversification in Madagascar: In situ radiation of two large C_3 shade clades and
1105 support for a Miocene to Pliocene origin of C_4 grassy biomes. *J. Biogeogr.* 45:750–761.
1106 Hafen T., Neveu H., Rumpler Y., Wilden I., Zimmermann E. 1998. Acoustically dimorphic
1107 advertisement calls separate morphologically and genetically homogenous populations of the
1108 grey mouse lemur (*Microcebus murinus*). *Folia Primatol.* 69:342–356.
1109 Harrison R. G., Larson E. L. 2014. Hybridization, introgression, and the nature of species
1110 boundaries. *J. Hered.* 105:795–809.
1111 Heckman K. L., Mariani C. L., Rasoloarison R., Yoder A. D. 2007. Multiple nuclear loci reveal
1112 patterns of incomplete lineage sorting and complex species history within western mouse
1113 lemurs (*Microcebus*). *Mol. Phylogenet. Evol.* 43:353–367.
1114 Heller R., Chikhi L., Sigiesmund H.R. 2013. The confounding effect of population structure on
1115 bayesian skyline plot inferences of demographic history. *PLoS ONE* 8:e62992.
1116 Herrera J. P., Dávalos L. M. 2016. Phylogeny and divergence times of lemurs inferred with recent
1117 and ancient fossils in the tree. *Syst. Biol.*65:772–791.
1118 Hey J., Nielsen R. 2007. Integration within the Felsenstein equation for improved Markov chain
1119 Monte Carlo methods in population genetics. *Proc. Natl. Acad. Sci. USA* 104:2785–2790.
1120 Hey J., Pinho C. 2012. Population genetics and objectivity in species diagnosis. *Evolution*
1121 66:1413–1429.
1122 Hotaling S., Foley M. E., Lawrence N. M., Bocanegra J., Blanco M. B., Rasoloarison R.,
1123 Kappeler P. M., Barrett M. A., Yoder A. D., Weisrock D. W. 2016. Species discovery and
1124 validation in a cryptic radiation of endangered primates: coalescent-based species
1125 delimitation in Madagascar's mouse lemurs. *Mol. Ecol.* 25:2029–2045.

1126 Huang J.-P., Leavitt S. D., Lumbsch H. T. 2018. Testing the impact of effective population size on
1127 speciation rates – a negative correlation or lack thereof in lichenized fungi. *Sci. Rep.* 8:5729.
1128 Hunnicutt K. E., Tiley G. P., Williams R. C., Larsen P. A., Blanco, M. B., Rasoloarison R. M.,
1129 Campbell C. R., Zhu K., Weisrock D. W., Matsunami H., Yoder A. D. 2019. Comparative
1130 genomic analysis of the pheromone receptor Class 1 family (V1R) reveals extreme
1131 complexity in mouse lemurs (genus, Microcebus) and a chromosomal hotspot across
1132 mammals. Gen. Biol. Evol. doi.org/10.1093/gbe/evz200
1133 Jackson N. D., Carstens B. C., Morales A. E., O'Meara B. C. 2017. Species delimitation with
1134 gene flow. *Syst. Biol.*66:799–812.
1135 Jombart T. 2008. adegenet: a R package for the multivariate analysis of genetic markers.
1136 *Bioinformatics* 24:1403–1405.
1137 Jombart T., Ahmed I. 2011. adegenet 1.3-1: new tools for the analysis of genome-wide SNP data.
1138 *Bioinformatics* 27:3070–3071.
1139 Kappeler P., Rasoloarison R., Razafimanantsoa L., Walter L., Roos C. 2005. Morphology,
1140 behaviour and molecular evolution of giant mouse lemurs (*Mirza* spp.) Gray, 1870, with
1141 description of a new species. *Primate Rep.* 71:3–26.
1142 Kass R. E., Raftery A. E. 1995. Bayes factors. *J. Am. Stat. Assoc.*90:773–795.
1143 Khatri B. S., Goldstein R. A. 2015. Simple biophysical model predicts faster accumulation of
1144 hybrid incompatibilities in small populations under stabilizing selection. *Genetics* 201:1525–
1145 1537.
1146 Khatri B. S., Goldstein R. A. 2018. Biophysics and population size constrains speciation in an
1147 evolutionary model of developmental system drift. *BioRxiv.* doi: 10.1101/123265.

Kiage L. M., Liu K. B. 2006. Late Quaternary paleo-environmental changes in East Africa: A review of multiproxy evidence from palynology, lake sediments, and associated records. *Prog. Phys. Geogr.* 30:633–658.

Kim B. Y., Wei X., Fitz-Gibbon S., Lohmueller K. E., Ortego J., Gugger P. F., Sork V. L. 2018. RADseq data reveal ancient, but not pervasive, introgression between Californian tree and scrub oak species (*Quercus* sect. *Quercus*: *Fagaceae*). *Mol. Ecol.* 27:4556–4571.

Knoop S., Chikhi L., Salmona J. 2018. Mouse lemur's use of degraded habitat. *Lemur News* 21:20–31.

Korneliussen T. S., Albrechtsen A., Nielsen R. 2014. Angsd: analysis of next generation sequencing data. *BMC Bioinformatics* 15:356.

Kottek M., Grieser J., Beck C., Rudolf B., Rubel F. 2006. World map of the Köppen-Geiger climate classification updated. *Meteorol. Z.*15:259–263.

Langmead B., Trapnell C., Pop M., Salzberg S. L. 2009. Ultrafast and memory-efficient alignment of short DNA sequences to the human genome. *Genome Biol.* 10:R25.

Leaché A., Zhu T., Rannala B., Yang Z. 2019. The spectre of too many species. *Syst. Biol.*68:168–181.

Leaché A. D., Fujita M. K., Minin V. N., Bouckaert R. R. 2014. Species delimitation using genome-wide SNP data. *Syst. Biol.*63:534–542.

Lecompte E., Crouau-Roy B., Aujard F., Holota H., Murienne J. 2015. Complete mitochondrial genome of the gray mouse lemur, *Microcebus murinus* (Primates, *Cheirogaleidae*). *Mitochondrial DNA A* 27:3514–3516.

Louis E. E., Coles M. S., Andriantompohavana R., Sommer J. A., Engberg S. E., Zaonarivelo J. R., Mayor M. I., Brenneman R. A. 2006. Revision of the mouse lemurs (*Microcebus*) of eastern Madagascar. *Int. J. Primatol.* 27:347–389.

1172 Louis E. E., Engberg S. E., McGuire S. M., McCormick M. J., Randriamampionona R.,
1173 Ranaivoarisoa J. F., Bailey C.A., Mittermeier R. A., Lei R. 2008. Revision of the mouse
1174 lemurs, *Microcebus* (Primates, Lemuriformes), of northern and northwestern Madagascar
1175 with descriptions of two new species at Montagne d'Ambre National Park and Antafondro
1176 Classified Forest. *Primate Conserv.* 23:19–38.
1177 Louis E. E., Lei R. 2016. Mitogenomics of the family *Cheirogaleidae* and relationships to
1178 taxonomy and biogeography in Madagascar. In: S. M. Lehman, U. Radespiel, and E.
1179 Zimmermann (Editors), *The Dwarf and Mouse Lemurs of Madagascar: Biology, Behavior*
1180 *and Conservation Biogeography of the Cheirogaleidae*, Chap. 3, Cambridge University
1181 Press, pp. 54–93.
1182 Lozier J. D. 2014. Revisiting comparisons of genetic diversity in stable and declining species:
1183 assessing genome-wide polymorphism in North American bumble bees using RAD
1184 sequencing. *Mol. Ecol.* 23:788–801.
1185 Luo A., Ling C., Ho S. Y. W., Zhu C. D. 2018. Comparison of methods for molecular species
1186 delimitation across a range of speciation scenarios. *Syst. Biol.*67:830–846.
1187 Maddison W. P. 1997. Gene trees in species trees. *Syst. Biol.*46:523–536.
1188 Mallet J., Besansky N., Hahn M. W. 2016. How reticulated are species? *BioEssays* 38:140–149.
1189 Markolf M., Brameier M., Kappeler P.M. 2011. On species delimitation: Yet another lemur
1190 species or just genetic variation? *BMC Evol. Biol*. 11:216.
1191 Martien K. K., Leslie M. S., Taylor B. L., Morin P. A., Archer F. I., Hancock-Hanser B. L.,
1192 Brittany L., Rosel P. E., Vollmer N. L. Viricel A., Cipriano F. (2017). Analytical approaches
1193 to subspecies delimitation with genetic data. *Mar. Mam. Sci.* 33:27-55.
1194 Martin R. 1972. A preliminary field-study of the lesser mouse lemur (*Microcebus murinus* JF
1195 Miller 1777). *Z. Tierpsychol.* 9:43–89.

1196 Matute D. R. 2013. The role of founder effects on the evolution of reproductive isolation. *J. Evol.*
1197 *Biol.* 26:2299–2311.
1198 Mayr E. 1959. Isolation as an evolutionary factor. *Proc. Am. Phil. Soc.* 103:221–230.
1199 Mazet O., Rodriguez W. V., Grusea S., Boitard S., Chikhi L. 2016. On the importance of being
1200 structured: instantaneous coalescence rates and human evolution – Lessons for inference of
1201 ancestral population size? *Heredity* 116:362–371.
1202 McCormack J. E., Heled J., Delaney K. S., Peterson A. T., Knowles L. L. 2011. Calibrating
1203 divergence times on species trees versus gene trees: implications for speciation history of
1204 *Aphelocoma jays*. *Evolution* 65:184–202.
1205 Meloro C., Cáceres N. C., Carotenuto F., Sponchiado J., Melo G. L., Passaro F., Raia P. 2015.
1206 Chewing on the trees: Constraints and adaptation in the evolution of the primate mandible.
1207 *Evolution* 69:1690–1700.
1208 Miller A., Mills H., Ralantoharijaona T., Volasoa N. A., Misandeau C., Chikhi L., Bencini R.,
1209 Salmona J. 2018. Forest type influences population densities of nocturnal lemurs in
1210 Manompana, northeastern Madagascar. *Int. J. Primatol.* 39:646–669.
1211 Myers N., Mittermeier R. A., Mittermeier C. G., Da Fonseca G. A., Kent J. 2000. Biodiversity
1212 hotspots for conservation priorities. *Nature* 403:853–858.
1213 Nater A., Mattle-Greminger M. P., Nurcahyo A., Nowak M. G., De Manuel M., Desai T., …,
1214 Lameira A. R. 2017. Morphometric, behavioral, and genomic evidence for a new orangutan
1215 species. *Current Biology* 27:3487-3498.
1216 Nielsen R., Korneliussen T., Albrechtsen A., Li Y., Wang J. 2012. SNP calling, genotype calling,
1217 and sample allele frequency estimation from new-generation sequencing data. *PLoS ONE*
1218 7:e37558.

1219 O'Leary S. J., Puritz J. B., Willis S. C., Hollenbeck C. M., Portnoy D. S. 2018. These aren't the
1220 loci you're looking for: Principles of effective SNP filtering for molecular ecologists. *Mol.*
1221 *Ecol.* 27:3193–3206.
1222 Olivieri G., Zimmermann E., Randrianambinina B., Rasoloharijaona S., Rakotondravony D.,
1223 Guschanski K., Radespiel U. 2007. The ever-increasing diversity in mouse lemurs: three new
1224 species in north and northwestern Madagascar. *Mol. Phylogenet. Evol.*43:309–327.
1225 Palkopoulou E., Lipson M., Mallick S., Nielsen S., Rohland N., Baleka S., Karpinski E.,
1226 Ivancevic A. M., To T. H., Kortschak R. D., Raison J. M., Qu Z., Chin T.-J., Alt K. W.,
1227 Claesson S., Dalén L., MacPhee R. D. E., Meller H., Roca A. L., Ryder O. A., Heiman D.,
1228 Young S., Breen M., Williams C., Aken B. L., Ruffier M., Karlsson E., Johnson J., Di Palma
1229 F., Alfoldi J., Adelson D. L., Mailund T., Munch K., Lindblad-Toh K. Hofreiter M., Poinar
1230 H., Reich D. 2018. A comprehensive genomic history of extinct and living elephants. *Proc.*
1231 *Natl. Acad. Sci. USA* 115:E2566–E2574.
1232 Pamilo P., Nei M. 1988. Relationships between gene trees and species trees. *Mol. Biol. Evol.*
1233 5:568–583.
1234 Pastorini J., Thalmann U., Martin R. D. 2003. A molecular approach to comparative
1235 phylogeography of extant Malagasy lemurs. *Proc. Natl. Acad. Sci. USA* 100:5879–5884.
1236 Patterson N., Moorjani P., Luo Y., Mallick S., Rohland N., Zhan Y., Genschoreck T., Webster T.,
1237 Reich D. 2012. Ancient admixture in human history. *Genetics* 192:1065–1093.
1238 Payseur B. A., Rieseberg L. H. 2016. A genomic perspective on hybridization and speciation.
1239 *Mol. Ecol.* 25:2337–2360.
1240 Pedersen C. E. T., Albrechtsen A., Etter P. D., Johnson E. A., Orlando L., Chikhi L., Siegismund
1241 H. R., Heller R. 2018. A southern African origin and cryptic structure in the highly mobile
1242 plains zebra. *Nat. Ecol. Evol.* 2:491–498.

1243 Quéméré E., Amelot X., Pierson J., Crouau-Roy B., Chikhi L. 2012. Genetic data suggest a
1244 natural pre-human origin of open habitats in northern Madagascar and question the
1245 deforestation narrative in this region. *Proc. Natl. Acad. Sci. USA* 109:13028–13033.
1246 R Core Development Team 2013. R: A Language and Environment for Statistical Computing. R
1247 Foundation for Statistical Computing, Vienna, Austria, URL. http://www.R-project.org/.
1248 Radespiel U. 2016. Can behavioral ecology help us to understand the divergent geographic range
1249 sizes of mouse lemurs? In: S. M. Lehman, U. Radespiel, and E. Zimmermann (Editors), *The*
1250 *Dwarf and Mouse Lemurs of Madagascar: Biology, Behavior and Conservation*
1251 *Biogeography of the Cheirogaleidae*, Chap. 26, Cambridge University Press, pp. 498-519.
1252 Radespiel U., Lutermann H., Schmelting B., Zimmermann E. (2019): An empirical estimate of
1253 the generation time of mouse lemurs. *Am. J. Primatol.* https://doi.org/10.1002/ajp.23062
1254 Radespiel U., Olivieri G., Rasolofoson D. W., Rakotondratsimba G., Rakotonirainy O.,
1255 Rasoloharijaona S., Randrianambinina B., Ratsimbazafy J. H., Ratelolahy F.,
1256 Randriamboavonjy T., Rasolofoharivelo T., Craul M., Rakotozafy L., Randrianarison R. M.
1257 2008. Exceptional diversity of mouse lemurs (*Microcebus* spp.) in the Makira region with the
1258 description of one new species. *Am. J. Primatol.* 70:1033–1046.
1259 Radespiel U., Ratsimbazafy J. H., Rasoloharijaona S., Raveloson H., Andriaholinirina N.,
1260 Rakotondravony R., Randrianarison R. M., Randrianambinina B. 2012. First indications of a
1261 highland specialist among mouse lemurs (*Microcebus* spp.) and evidence for a new mouse
1262 lemur species from eastern Madagascar. *Primates* 53:157–170.
1263 Radespiel U., Sarikaya Z., Zimmermann E., Bruford M.W. (2001) Sociogenetic structure in a
1264 free-living nocturnal primate population: sex-specific differences in the grey mouse lemur
1265 (*Microcebus murinus*). *Behav. Ecol. Sociobio*. 50:493-502.

Rannala B., Yang Z. 2003. Bayes estimation of species divergence times and ancestral population sizes using DNA sequences from multiple loci. *Genetics* 164:1645–1656.

Rannala B., Yang Z. 2013. Improved reversible jump algorithms for Bayesian species delimitation. *Genetics* 194:245–253.

Rasoloarison R. M., Goodman S. M., Ganzhorn J. U. 2000. Taxonomic revision of mouse lemurs (*Microcebus*) in the western portions of Madagascar. *Int. J. Primatol.* 21:963–1019.

Rasoloarison R. M., Weisrock D. W., Yoder A. D., Rakotondravony D., Kappeler P. M. 2013. Two new species of mouse lemurs (*Cheirogaleidae*: *Microcebus*) from eastern Madagascar. *Int. J. Primatol.* 34:455–469.

Rice W. R., Hostert E. E. 1993. Laboratory experiments on speciation: What have we learned in 40 years? *Evolution* 47:1637–1653.

Rodríguez W., Mazet O., Grusea S., Arredondo A., Corujo J. M., Boitard S., Chikhi L. 2018. The IICR and the non-stationary structured coalescent: towards demographic inference with arbitrary changes in population structure. *Heredity* 121:663-678.

Schiffels S., Durbin R. 2014. Inferring human population size and separation history from multiple genome sequences. *Nat. Genet.* 46:919–925.

Schüßler D., Mantilla-Contreras J., Stadtmann R., Ratsimbazafy J. H., Radespiel U. (in revision) Determinants of deforestation and prediction of future forest loss in remote and rural north-eastern Madagascar. *Biodiv. Conserv*.

Schüßler D., Radespiel U., Ratsimbazafy J.H., Mantilla-Contreras J. 2018. Lemurs in a dying forest: Factors influencing lemur diversity and distribution in forest remnants of north-eastern Madagascar. *Biol. Conserv.* 228:17–26.

Skotte L., Korneliussen T. S., Albrechtsen A. 2013. Estimating individual admixture proportions from next generation sequencing data. *Genetics* 195:693–702.

1290 Solís-Lemus C., Knowles L. L., Ané C. (2015). Bayesian species delimitation combining
1291 multiple genes and traits in a unified framework. *Evol*. 69:492-507.
1292 Stamatakis A. 2014. Raxml version 8: a tool for phylogenetic analysis and post-analysis of large
1293 phylogenies. *Bioinformatics* 30:1312–1313.
1294 Struck T.H., Feder J.L., Bendiksby M., Birkeland S., Cerca J., Gusarov V.I., Kistenich S., Larsson
1295 K.H., Liow L.H., Nowak M.D., Stedje B., Bachmann L., Dimitrov D. 2018. Finding
1296 Evolutionary Processes Hidden in Cryptic Species. *Trends Ecol. Evol*. 33:153-163.
1297 Sukumaran J., Knowles L. L. 2017. Multispecies coalescent delimits structure, not species. *Proc.*
1298 *Natl. Acad. Sci. USA* 114:1607–1612.
1299 Tattersall I. 2007. Madagascar's lemurs: Cryptic diversity or taxonomic inflation? *Evol. Anthr*.
1300 16:12-23.
1301 Uyeda J. C., Arnold S. J., Hohenlohe P. A., Mead L. S. 2009. Drift promotes speciation by sexual
1302 selection. *Evolution* 63:583–594.
1303 Venables W. N., Ripley B. D. 2002. *Modern Applied Statistics with S.* Fourth Edition. Springer,
1304 New York. ISBN 0-387-95457-0. URL http://www.stats.ox.ac.uk/pub/MASS4
1305 Viguier B. 2004. Functional adaptations in the craniofacial morphology of Malagasy primates:
1306 shape variations associated with gummivory in the family *Cheirogaleidae*. *Ann. Anat.*
1307 186:495–501.
1308 Vorontsova M. S., Besnard G., Forest F., Malakasi P., Moat J., Clayton W. D., Ficinski P., Savva
1309 G. M., Nanjarisoa O. P., Razanatsoa J., Randriatsara F. O., Kimeu J. M., Luke W. R. Q.,
1310 Kayombo C., Linder H. P. 2016. Madagascar’s grasses and grasslands: Anthropogenic or
1311 natural? *Proc. Roy. Soc. B* 283:20152262.

1312 Waeber P. O., Wilmé L., Mercier J. R., Camara C., Lowry II P. P. 2016. How effective have thirty
1313 years of internationally driven conservation and development efforts been in Madagascar?
1314 *PLoS ONE* 11:e0161115.
1315 Warmuth V. M., Ellegren H. 2019. Genotype-free estimation of allele frequencies reduces bias
1316 and improves demographic inference from RADSeq data. *Mol. Ecol. Resour.* 19:586–596.
1317 Weisrock D. W., Rasoloarison R. M., Fiorentino I., Ralison J. M., Goodman S. M., Kappeler
1318 P. M., Yoder A. D. 2010. Delimiting species without nuclear monophyly in Madagascar's
1319 mouse lemurs. *PLoS ONE* 5:e9883.
1320 Wen D., Yu Y., Zhu J., Nakhleh L. 2018. Inferring phylogenetic networks using PhyloNet. *Syst.*
1321 *Biol.* 67:735–740.
1322 Wilmé L., Goodman S. M., Ganzhorn J. U. 2006. Biogeographic evolution of Madagascar's
1323 microendemic biota. *Science* 312:1063–1065.
1324 Xie W., Lewis P. O., Fan Y., Kuo L., Chen M. H. 2011. Improving marginal likelihood estimation
1325 for Bayesian phylogenetic model selection. *Syst. Biol.* 60:150–160.
1326 Yang Z., Rannala B. 2010. Bayesian species delimitation using multilocus sequence data. *Proc.*
1327 *Natl. Acad. Sci. USA* 107:9264–9269.
1328 Yang Z., Yoder A. D. 2003. Comparison of likelihood and Bayesian methods for estimating
1329 divergence times using multiple gene loci and calibration points, with application to a
1330 radiation of cute-looking mouse lemur species. *Syst. Biol.* 52:705–716.
1331 Yoder A. D., Campbell C. R., Blanco M. B., dos Reis M., Ganzhorn J. U., Goodman S. M.,
1332 Hunnicutt K. E., Larsen P. A., Kappeler P. M., Rasoloarison R. M., Ralison J. M., Swofford
1333 D. L., Weisrock D. W. 2016. Geogenetic patterns in mouse lemurs (genus *Microcebus*) reveal
1334 the ghosts of Madagascar's forests past. *Proc. Natl. Acad. Sci. USA* 113:8049–8056.

1335 Yoder A. D., Rasoloarison R. M., Goodman S. M., Irwin J. A., Atsalis S., Ravosa M. J., Ganzhorn
1336 J. U. 2000. Remarkable species diversity in Malagasy mouse lemurs (*Primates*, *Microcebus*).
1337 *Proc. Natl. Acad. Sci. USA* 97:11325–11330.
1338 Zimin A. V., Marçais G., Puiu D., Roberts M., Salzberg S. L., Yorke J. A. 2013. The MaSuRCA
1339 genome assembler. *Bioinformatics* 29:2669–2677.
1340 Zimmermann E., Cepok S., Rakotoarison N., Zietemann V., Radespiel U. 1998. Sympatric mouse
1341 lemurs in north-west Madagascar: A new rufous mouse lemur species (*Microcebus*
1342 *ravelobensis*). *Folia Primatol.* 69:106–114.
1343 Zimmermann E., Radespiel U. 2014. Species concepts, diversity, and evolution in primates:
1344 lessons to be learned from mouse lemurs. *Evol. Anthropol.* 23:11–14.